

**UNIVERSITA' DEGLI STUDI DI NAPOLI
"FEDERICO II"**

FACOLTA' DI FARMACIA

Dipartimento di Farmacologia Sperimentale

**TESI DI DOTTORATO DI RICERCA
IN SCIENZA DEL FARMACO**

XIII CICLO



**DIVERGENT MODULATION OF IRON
REGULATORY PROTEINS AND FERRITIN
BIOSYNTHESIS BY HYPOXIA/REOXYGENATION
IN NEURONS AND GLIAL CELLS**

TUTORE
Chiar.mo Prof.
Rita Santamaria

COORDINATORE
Chiar.mo Prof.
Enrico Abignente

DOTTORANDA
Dott. Carmen Maffettone

2002-2005

ACKNOWLEDGMENTS

I would like to thank many of the special people who assisted me through the completion of the thesis.

First, my sincere gratitude goes to my supervisor Prof. Rita Santamaria for her guidance, encouragement and great support through the past three years. I am also thankful to Prof. Alfredo Colonna for his constant assistance, for financial support and for his great encouragements. Their invaluable advices and constant supervisions were indispensable for my research work and my scientific formation.

Gratitude also goes to Prof. Francesco Capasso, chief of the Department of Experimental Pharmacology, and to Prof. Enrico Abignente, director of my PhD.

I wish to express my gratitude to Dr. Carlo Irace for his assistance and friendship in the laboratory and to all colleagues for their continuous support.

This Doctorate thesis is dedicated to my family, to my grandparents and to my uncle Felicetto. Thanks for you care, love, encouragement and confidence in me for all these years.

SUMMARY

Neuronal and glial cells require iron for DNA synthesis and mitochondrial respiration and as cofactor for enzymes involved in neurotransmitters synthesis and axon myelination (Chen *et al.*, 1995; Connor and Menzies, 1996). In addition, free iron can promote the generation of reactive oxygen species via Haber Weiss-Fenton reactions thereby leading to lipid, protein and DNA damage (Halliwell and Gutteridge, 1990). The maintenance of iron homeostasis is mainly regulated by the transferrin receptor that transports iron into the cell

(Fishman *et al.*, 1987) and by ferritin that sequesters this metal (Harrison and Arosio, 1996). The level of ferritin is mainly regulated post-transcriptionally by interaction between the iron regulatory proteins IRP1 and IRP2 and a sequence located in the 5' untranslated region of ferritin mRNA (iron responsive element, IRE). IRP1, the cytosolic counterpart of mitochondrial aconitase (Kennedy *et al.*, 1992), is a bifunctional protein that, through [4Fe-4S] cluster assembly/disassembly, switches from the aconitase form to the IRP1 form in response to the intracellular iron level (Guo *et al.*, 1994). IRP2,

homologous to IRP1, lacks the [4Fe-4S] cluster and its activity increases in iron-depleted cells by protein stabilization.

Dysregulation of iron homeostasis coupled to oxidative stress occurs in several neurodegenerative disorders (Thompson *et al.*, 2001; Ke and Ming Qian, 2003), as well as in ischemic brain injury (Kondo *et al.*, 1995; Dorrepaal *et al.*, 1996). Furthermore, induction of ferritin immunoreactivity and activation of ferritin gene transcription has been shown in the brain during ischemia/reperfusion (Ishimaru *et al.*, 1996; Chi *et al.*, 2000).

Given the susceptibility of cerebral cells to iron-induced oxidative stress, we investigated the intracellular mechanisms that control ferritin synthesis and ferritin's role as an iron-segregating protein in the cell's defense against hypoxia/reoxygenation-induced injury. We thus examined IRP RNA-binding activity, ferritin expression and biosynthesis in cortical neurons and glial cells exposed to oxygen and glucose deprivation (OGD¹), and to OGD followed by reoxygenation.

The results show that hypoxia decreases IRP1 binding activity in glial cells and enhances it in cortical neurons. These effects were reversed by reoxygenation in both cell types. In glial cells there was an early increase of ferritin synthesis during the hypoxia and

reoxygenation, and baseline level was reached within 24 hr. Conversely, in cortical neurons ferritin synthesis was stimulated only during the late phase of reoxygenation. Analysis of ferritin mRNA levels, suggests that ferritin synthesis in glial cells is regulated mainly post-transcriptionally by IRPs, while the late ferritin increase in neurons is IRPs-independent and seems to be transcriptionally regulated. The different regulation of ferritin expression may account for the different vulnerability of neurons and glial cells to the injury elicited by oxygen and glucose deprivation/reoxygenation.

The greater vulnerability of cortical neurons to hypoxia-reoxygenation was strongly attenuated by exogenous administration of ferritin during OGD/reoxygenation, suggesting the possible cytoprotective role exerted by this iron-segregating protein.

TABLE OF CONTENTS

ACKNOWLEDGMENTS.....	1
LIST OF FIGURES.....	9
LIST OF TABLES.....	11

Introduction

1. The importance of iron.....	12
1.1 Iron- an essential but potentially toxic nutrient.....	12
1.2 Toxicity of iron.....	13
1.3 Iron in the brain.....	16
1.4 Mechanisms of iron transport in the brain.....	18
1.5 Cellular iron uptake	22
1.6 Cellular iron use.....	26
1.7 Ferritin structure and function.....	29
1.8 Ferritin in the brain.....	32
2 . Cytoplasmatic control of ferritin synthesis.....	35
2.1 Iron-mediated regulation of ferritin.....	35
2.2 IRP1 and IRP2.....	36

2.3 IRP regulation by stimuli other than iron.....	41
3. Hypoxia.....	43
3.1 Regulation of HIF-1.....	47
3.1.1 Oxygen-dependent.....	47
3.1.2 Oxygen-independent.....	48
3.2 Hypoxia-mediated iron regulation.....	49
3.3 Ferritin regulation during hypoxia-ischemia.....	50
3.4 How would hypoxia regulate iron metabolism?.....	52
<u>4.0 Materials and Methods</u>	
4.1 Animals.....	57
4.2 Primary cortical neuronal cultures.....	57
4.3 Primary glial cell cultures.....	58
4.4 Glioma cells	59
4.5 Combined oxygen and glucose deprivation and reoxygenation.....	59

4.6 Permanent middle cerebral artery occlusion (pMCAO) and identification of the ischemic area.....	60
4.7 Preparation of cytosolic and mitochondrial extracts.....	62
4.8 Electrophoretic mobility-shift assay (EMSA).....	63
4.9 Western blot analysis.....	65
4.10 Metabolic labeling with ³⁵ S-methionine/cysteine and immunoprecipitation.....	66
4.11 RNA extraction and Northern blot analysis.....	67
4.12 Cell viability assay.....	69
4.13 Lipid peroxidation assay.....	70
4.14 Apoferritin treatment of cortical neurons.....	71
4.15 Statistical analysis.....	72

5.0 Results

5.1 IRP RNA-binding activity in cortical neurons and in glial cells after OGD.....	73
5.2 Response of IRP2 to iron concentration during OGD.....	76
5.3 IRP RNA-binding activity during OGD followed by reoxygenation.....	78
5.4 Effects of OGD and OGD/reoxygenation on ferritin expression.....	80

5.5 Effects of OGD and OGD/reoxygenation on ferritin biosynthesis.....	83
5.6 Analysis of H-ferritin mRNA levels after OGD and OGD/reoxygenation.....	83
5.7 In vivo cerebral ischemia modulates IRP-RNA binding and affects ferritin levels.....	84
5.8 Effects of OGD and OGD/reoxygenation on lipid peroxidation and on survival of cortical neurons and glial cells.....	88
5.9 Effect of exogenous ferritin addition on lipid peroxidation in cortical neurons exposed to OGD followed by reoxygenation.	91
<u>6.0 Discussion and Conclusions</u>	95
<u>7.0 References</u>	104

LIST OF FIGURES

Fig. 1. Iron and free radical.....	14
Fig. 2. Proposed scheme for iron transport across the BBB.....	19
Fig. 3. Proposed scheme for iron transport in the brain.....	21
Fig. 4. The Tf cycle.....	23
Fig. 5. Ferritin structure.....	30
Fig. 6. Homeostatic responses to iron supply mediated by IRE-IRP interactions.....	37
Fig. 7. IRPs regulation by iron and other stimuli.....	38
Fig. 8. Hypoxia and iron metabolism.....	53
Fig. 9. IRP1 and IRP2 RNA-binding activity in rat cerebral cells during OGD.....	74
Fig. 10. Response of IRPs to intracellular iron concentration during OGD.....	77
Fig. 11 IRP1 and IRP2 RNA-binding activity in rat cerebral cells during reoxygenation.....	79
Fig. 12. Effects of OGD and OGD/Reoxy on cellular ferritin levels.....	81
Fig. 13. Ferritin synthesis during OGD and OGD/Reoxy.....	82
Fig. 14 Northern blot analysis for H-ferritin mRNA levels.....	85
Fig. 15. Effects of OGD and OGD/reoxygenation on survival of cortical neurons and glial cells.....	86
Fig. 16. Effects of OGD and OGD/reoxygenation on free radical production in cortical neurons and glial cells.....	87

Fig. 17. Western blot analysis for cytochrome c release and for pro-caspase-3 cleavage.....89

Fig. 18. Ferritin effect on lipid peroxidation in cortical neurons exposed to OGD followed by reoxygenation.....92

Fig. 19. Effects of *in vivo* cerebral ischemia on IRPs RNA-binding and ferritin levels.....94

LIST OF TABLES

Table. 1. Effects of OGD and OGD/reoxygenation on free radical production and on survival of cortical neurons and glial cells.....	90
---	-----------

INTRODUCTION

1. The importance of iron

1.1 Iron: an essential but potentially toxic nutrient

The chemical versatility of iron has made it one of the most commonly used metals in biological system. In vertebrates, multiple physiological processes including oxygen transport, respiration, DNA synthesis, formation of some neurotransmitters and hormones, xenobiotics metabolism, and certain aspects of host defense use iron-containing proteins.

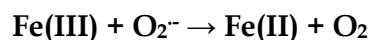
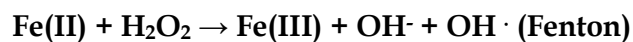
The essential role of iron in human and animal health became apparent with the identification of iron as body constituent and with the understanding of the relationship between adequate iron intake and the prevention of certain diseases (Neilands, 1991). Today, the nutritional importance of iron is clear, given the worldwide prevalence of physiological disorders arising from iron deficiency and the demonstration of the central role of iron-containing proteins in multiple cellular processes (Bothwell, 1995). However, when present at levels that exceed the capacity of organism to safely use it,

iron can be toxic because of its ability to promote oxidation of lipids, proteins, and other cellular components. High levels of iron have been associated with increased incidence of some cancers, dysfunction of organs, such as heart, pancreas, or liver and development of neurodegenerative disorders (Halliwell, 1992).

1.2 Toxicity of iron

The efficiency of Fe(II) as an electron donor and of Fe(III) as an electron acceptor is a fundamental feature for many biochemical reactions and renders this element an essential mineral and nutrient. However, this property turns iron into a potential biohazard, because under aerobic conditions, it can readily catalyze the generation of noxious radicals. Iron's toxicity is largely based on Fenton and Haber-Weiss chemistry (Fig. 1A), where catalytic amounts of iron are sufficient to yield hydroxyl radicals ($\text{OH}\cdot$) from superoxide ($\text{O}_2^{\cdot-}$) and hydrogen peroxide (H_2O_2), collectively known as "reactive oxygen intermediates" (ROIs) (Halliwell and Gutteridge, 1990). Importantly,

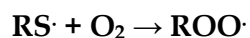
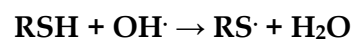
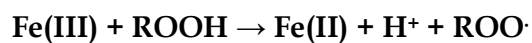
A.



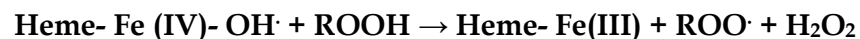
Net reaction:



B.



C.



D.

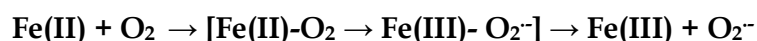
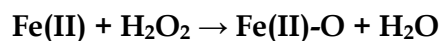


Fig. 1. Iron and free radical

(A) Iron-catalyzed generation of the hydroxyl radical via the Fenton reaction; the net Haber-Weiss reaction is also indicated. (B) Iron-catalyzed generation of organic radicals. (C) Heme-catalyzed generation of oxygen radicals via oxoferryl intermediates. (D) Direct interaction of iron with oxygen.

ROIs are inevitable byproducts of aerobic respiration and emerge by incomplete reduction of dioxygen in mitochondria. ROIs can also be generated during enzymatic reactions in other subcellular compartments, such as in peroxisomes, the endoplasmic reticulum, or the cytoplasm.

Redox active iron catalyzes the generation of not only hydroxyl radicals, but also of organic reactive species, such as peroxy ($\text{ROO}\cdot$), alkoxy ($\text{RO}\cdot$), thiyl ($\text{RS}\cdot$), or thiyl-peroxy ($\text{RSOO}\cdot$) radicals (fig. 1B). Interestingly, heme iron may also catalyze the formation of radicals, mainly via formation of oxoferryl intermediates (Ryter and Tyrrell, 2000) (fig. 1C). Finally, ferrous iron can also contribute as reactant, rather than as catalyst, to free radical generation by a direct interaction with oxygen, via ferryl ($\text{Fe}^{2+}\text{-O}$) or perferryl ($\text{Fe}^{2+}\text{-O}_2$) iron intermediates.

Free radicals are highly reactive species and may promote oxidation of proteins, peroxidation of membrane lipids, and modification of nucleic acids. An increase in the steady state levels of reactive oxygen species beyond the antioxidant capacity of the organism, called oxidative stress, is encountered in many pathological conditions, such as chronic inflammation, ischemia-reperfusion injury, or neurodegeneration (Ischiropoulos and Beckman, 2003). Excess of

redox active iron aggravates oxidative stress and leads to accelerated tissue degeneration. This is evident in disorders of hereditary or secondary iron overload. Under physiological conditions, extracellular iron is exclusively bound to transferrin, a monomeric glycoprotein serving as the plasma iron carrier, which maintains iron soluble and non-toxic, unable to engage in Fenton/Haber-Weiss reactions (Ponka *et al.*,1998). In healthy individuals, only 30% of circulating transferrin binds to iron. In pathological iron overload, iron gradually saturates the iron-binding capacity of transferrin and forms redox-active, low-molecular-weight chelates. Non-transferrin-bound iron eventually gets internalized into tissues by poorly defined mechanisms, resulting in cell damage and tissue injury.

1.3 Iron in the brain

Iron is the most abundant transition metal in the brain. It not only acts as cofactor for many heme and non-heme enzymes involved in cellular energy metabolism, but it also plays an essential role in many other metabolic processes including DNA and protein synthesis, formation of myelin and of dopamine and development of dendritic trees (Gerlach *et al.*, 1994). In the brain, iron is most

abundant in the basal ganglia (at a concentration equivalent to that in the liver, the third most abundant source of iron in the body) (Beard *et al.*, 1993).

Iron is predominantly stored within oligodendrocytes, cells of the CNS that produce and maintain myelin. Indeed, iron-containing oligodendrocytes are found in satellite positions near large neurons where they regulate iron availability to neurons.

The iron transport protein, transferrin (Tf), is also predominantly found in the oligodendrocytes, but additional locations include tanycytes, endothelial cells, choroids plexus, epithelial cells, and ependymal cells (Connor, 1994). It is notable that iron and Tf are not distributed identically in the brain because Tf are not the main storage form of iron. Ferritin (Fr), a multimeric protein that binds up to 4500 atoms, is the major storage form of iron. Indeed, there is 10 times more ferritin than transferrin in the cerebral cortex. About one-third of brain iron is stored in ferritin in the ferric form (Fe^{3+}), which is also predominantly distributed in glial cells, particularly in microglia and oligodendrocytes (Morris *et al.*, 1992). It is evident that oligodendrocytes play an important role in maintaining iron homeostasis in the brain.

1.4 Mechanisms of iron transport in the brain

The mechanisms of iron transport across the blood-brain-barrier (BBB) have not yet been completely clarified. Evidences suggests that the transferrin-transferrin receptor (Tf-TfR) pathway might be the major route of iron transport across the luminal membrane of the capillary endothelium (Malecki *et al.*, 1999), and that iron, possibly in the form of Fe^{2+} , crosses the abluminal membrane and enters the interstitial fluid(IF). However, the molecular events of this process are not known. Evidence shows that the uptake of Tf-bound iron (Tf-Fe) by TfR-mediated endocytosis from the blood into the cerebral endothelial cells is no different from uptake into other cells types (Bradbury, 1997). This processes includes several steps: binding, endocytosis, acidification and dissociation, then translocation of the iron across the endosomal membrane, by a processes mediated by divalent metal transporter 1 (DMT1) (Burdo *et al.*, 2001). Most of the Tf will return to the luminal membrane with TfR, whereas the iron crosses the abluminal membrane by undetermined mechanism (fig. 2). Recent studies have shown that ferroportin 1-hephaestin (FP1-Hp) and/or Hp-independent iron export systems might play a key role in Fe^{2+} transport across the basal membrane of enterocytes in the

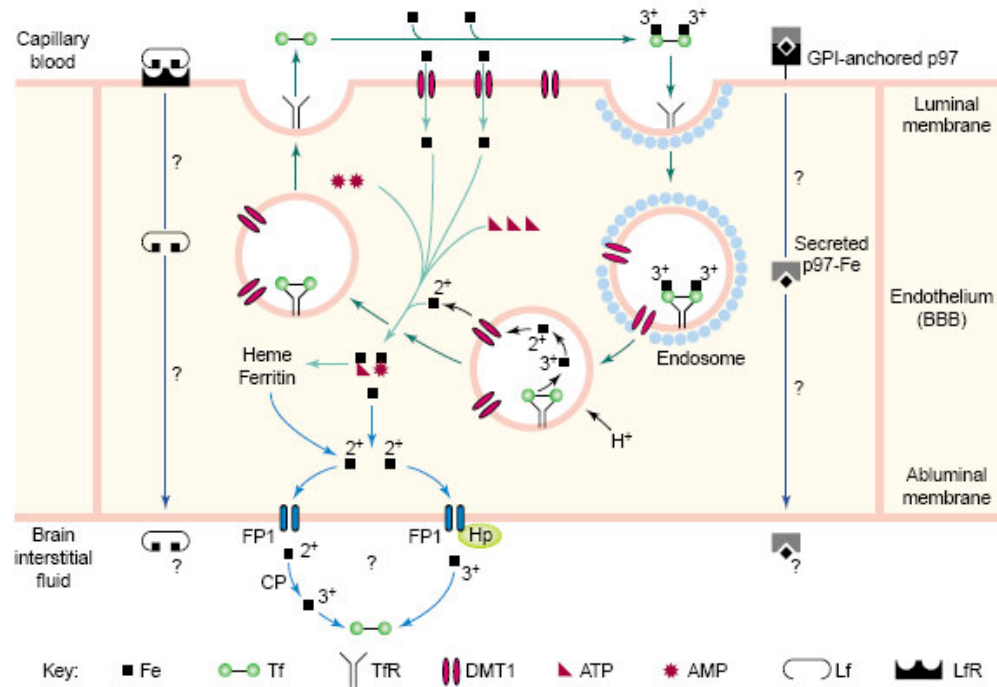


Fig. 2. Proposed scheme for iron transport across the BBB

The Tf-TfR pathway might be the major route of iron transport across the luminal membrane of the BBB. Tf-Fe uptake by endothelial cells is similar in nature to the uptake into other cell types (green arrows). Iron (Fe^{2+}) probably crosses the abluminal membrane via FP1-Hp and/or independent export system (light blue arrows). Lfr-Lf and GPI-anchored p67-secreted-p97 pathway might also be involved in iron transport across the BBB (dark blue arrows).

Abbreviations: BBB, brain-blood barrier; Cp, ceruloplasmin; DMT1, divalent metal transporter; FP1, ferroportin 1; GPI-p97, GPI-anchored p97; Hp, hephastin; Lf, lactoferrin; LfR, lactoferrin receptor; NTBI, non-transferrin-bound iron; Tf-Fe, transferrin-bound iron; Tf, transferrin; TfR, transferrin receptor.

gut (Donovan *et al.*, 2000; Vulpe *et al.*, 1999), but it is unknown if these two systems have the same role in Fe²⁺ transport across the abluminal membrane of BBB.

Another proposed mechanism of Fe²⁺ transport across abluminal membrane involves astrocytes that probably have the ability to take up Fe²⁺ from endothelial cells (Oshiro *et al.*, 2000). In addition to the Tf-TfR pathway, it has been suggested that the lactoferrin receptor-lactoferrin (LfR-Lf) and glycosylphosphatidylinositol (GPI)-anchored p97-secreted p97 pathways might also play a role in iron transport across the BBB (Faucheux *et al.*, 1995). It is also possible that a small amount of iron might cross the BBB in the form of intact Tf-Fe complex by receptor-mediated transcytosis (Moos *et al.*, 1998) (fig. 2). After the transport across the BBB the iron binds quickly to Tf that is secreted from oligodendrocytes and epithelial cells of the choroids plexus (Moos *et al.*, 1998) (fig.3). Because the affinity of Tf with iron is higher than that of the other iron transporters, Fe³⁺ in CSF and IF will bind to Tf first. Unlike Tf in blood, Tf in CSF and IF is fully saturated with iron and the excess of iron will bind to other transporters. Hence, it is possible that there are two transport forms

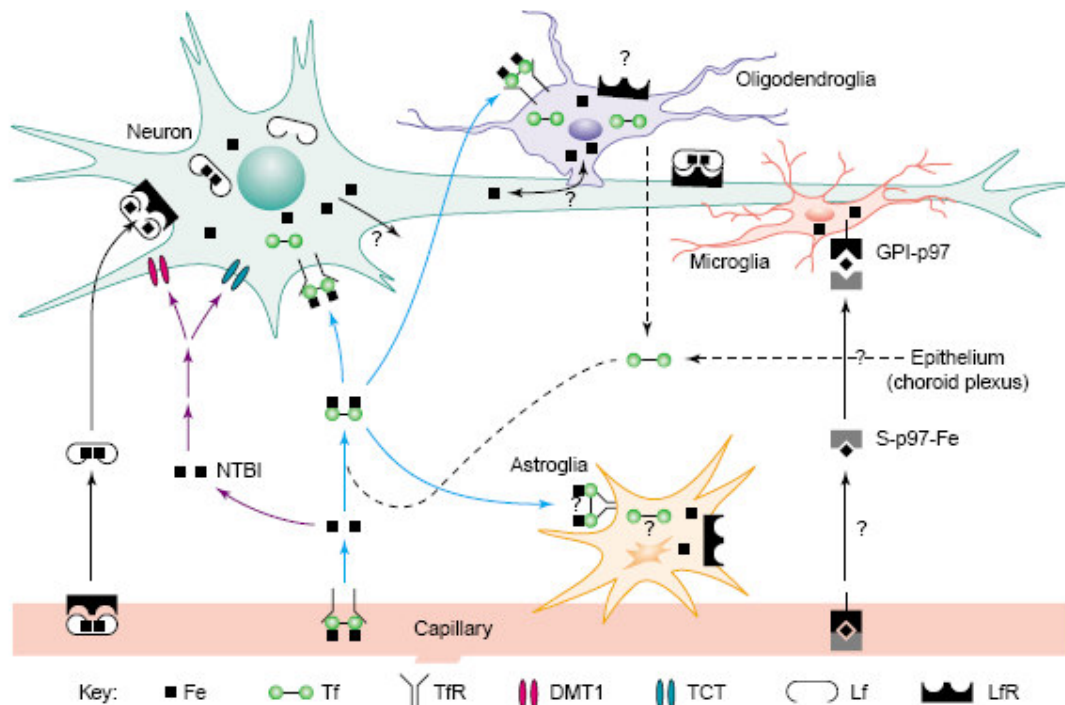


Fig. 3. Proposed scheme for iron transport in the brain

There are two transport forms of iron in the brain: Tf-Fe and NTBI. Tf-Fe is taken up by neurons via a TfR-mediated (blue arrows) process. NTBI, including Lf-Fe³⁺ and S-p97-Fe³⁺, is acquired by neurons probably via DMT1- and TCT-mediated (purple arrows) processes or LfR and GPI-p97-mediated processes (black arrows). The molecular mechanism underlying these processes are unknown.

Abbreviations: DMT1, divalent metal transporter; GPI-p97, GPI-anchored p97; LfR, lactoferrin receptor; NTBI, non-transferrin-bound iron; S-p97, secreted p97; TCT, trivalent cation-specific transporter; Tf-Fe, transferrin-bound iron; Tf-Fe, transferrin-bound iron; Tf-TfR, transferrin-transferrin receptor.

of iron in the CSF and IF in the brain: Tf-Fe and non-Tf-bound iron (NTBI) (Moos *et al.*, 1998). The latter probably includes citrate- Fe³⁺, ascorbate- Fe²⁺ and albumin-Fe (2+ or 3+), as well as Lf- Fe³⁺ and secreted p-97- Fe³⁺.

Tf-Fe, or probably Lf-Fe, and secreted p97-Fe will be taken up by brain cells via TfR- or Lfr- and GPI-anchored p-97-mediated processes, respectively (Malecki *et al.*, 1999). NTBI will be acquired by neuronal cells or other brain cells, probably via DMT-1- or trivalent cation-specific transporter (TCT)-mediated mechanism.

1.5 Cellular iron uptake

Transferrin receptor provides for controlled access of transferrin to cells (fig.4). Two such receptors have been described. The first and much more studied of these is now known as transferrin receptor 1 (TfR1). Consisted of two disulfide-bonded identical 90 KDa subunits, each bearing three asparagines-linked and one threonine-linked carbohydrate chains, TfR is expressed by all iron-requiring cells, and is far more abundant than transferrin receptor 2 (TfR2). The first 61 amino acids of each subunit form the cytoplasmatic domain, and lead to a membrane-anchoring hydrophobic sequence of residues 62-

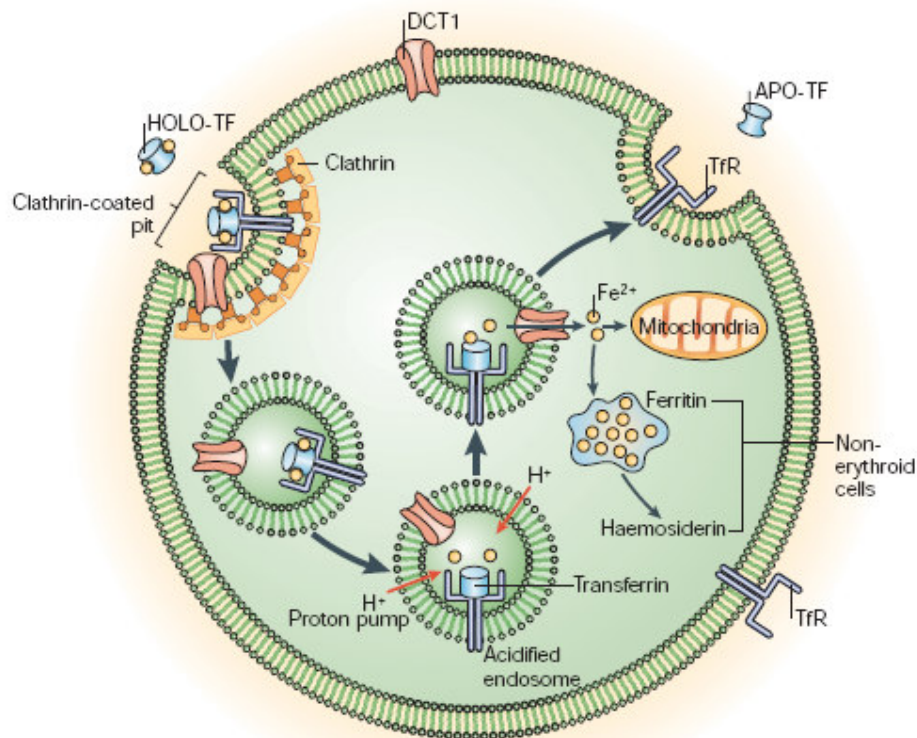


Fig. 4. The Tf cycle

Holotransferrin (HOLO-Tf) binds to the transferrin receptor (TfR) at the cell surface. These complexes localize to clathrin-coated pits, which invaginate to initiate endocytosis. Specialized endosomes form, which are acidified by a proton pump. When the required acidic pH is reached, iron is released from transferrin (Tf) and is co-transported, with the protons, out of the endosomes by the divalent cation transporter DCT1. Apotransferrin (APO-Tf) is returned to the cell membrane bound to TfR, where, at neutral pH, they dissociate to participate in further rounds of iron delivery. The iron can be targeted to the mitochondria. In non-erythroid cells, iron is stored in the form of ferritin and haemosiderin.

89 that spans the lipid bilayer once. The remainder of the protein, bearing the transferrin recognition sites, lies in the exocytic region. TfR2, described in 1999, exists in two forms. The first of these, TfR2- α , has 45% sequence identity and 66% similarity to TfR1, while the second, TfR2- β , lacks the N-terminal portion, including the cytoplasmic and transmembrane regions. Expression of TfR2 is predominantly in liver and liver-derived cell lines, but also in human erythroleukemic K562 cells.

Tf binds to the TfR at the cell surface and is internalized through clathrin-coated pits into endosomes via a well characterized pathway (fig. 4). At the acidic pH of the endosome, iron dissociates from Tf and is taken to the cytoplasm, presumably via a membrane transporter. The rate of iron release from Tf to cells depends on the pH of the endosome and its association with the TfR (Sipe *et al.*, 1991), but the efficiency is probably less than 100%. Endosomal pH varies with cell type, ranging from 6 to 5.5. Even the lowest pH achieved by endosomes, however, is not sufficient to remove iron from transferrin in the few minutes taken by the transferrin cycle, so that other mechanisms must participate in iron release. Such mechanisms might include the availability of iron-sequestering

molecules such as citrate or ATP, or the reduction of iron in the transferrin-transferrin receptor complex, as suggested by recent identification of a membrane ferrireductase (McKie *et al.*, 2001). Further characterization of the trafficking of ferrireductase is needed to explore this possibility. After the return of the receptor Tf complex to the cell surface, the extracellular pH triggers the release of apo-Tf, allowing another round of binding and endocytosis to begin.

The transferrin/TfR1 pathway defines the major route for cellular iron uptake and some cell types (for example erythroid cells) depend on it for iron acquisition. The targeted disruption of mouse TfR1 has been associated with early embryonic lethality due to defective erythropoiesis (Levy *et al.*, 1999). Transferrin receptor 2 (TfR2), an homologue of TfR1, cannot compensate for TfR1 deficiency and rescue the embryonic lethal phenotype of TfR1 ^{-/-}. The defect in TfR1 ^{-/-} embryos is restricted within the erythroid and neuronal tissue (Levy *et al.*, 1999), suggesting that alternative pathway for cellular iron acquisition in other types exist. For example, new pathway for the delivery of iron into cells via enterobactin and the neutrophil-derived protein neutral gelatinase-associated lipocalin (NGAL) has recently been described (Goetz *et al.*, 2002; Yang *et al.*, 2002).

Enterobactin belongs to a class of low-molecular-weight iron-chelating metabolites known as siderophores, which are synthesized by some bacteria and fungi to scavenge extracellular iron. It is not clear whether mammals can produce siderophores themselves, but the above data suggest that they can utilize siderophore-based mechanisms for iron acquisition.

1.6 Cellular iron use

Once iron has entered the cytosol, little is known about how it is shuttled to the various intracellular proteins and organelles that need iron. Generally, there are three possible fates for iron in the cytoplasm: a) it is used for the synthesis of iron-containing proteins; b) it is stored; or c) it is exported from the cells. The extent to which iron delivered to the cytoplasm is then directed, along metabolic pathways, rather than being incorporated into the iron storage proteins, likely depends on the amount of iron taken up, as well as the iron status and metabolic needs of the cells. One critical location of intracellular iron use is the mitochondrion. This organelle is the site of iron incorporation into protoporphyrin IX to form heme, as well as the location where metal centers for heme and/or non heme

are assembled and inserted into proteins required for mitochondrial function. In liver and in erythroid cells, a large fraction of iron is used for heme formation that is modulated by coordinating the synthesis of protoporphyrin IX with the availability of iron (Ponka *et al.*, 1997). The rate-limiting enzyme for heme formation is 5-aminolevulinate synthase (eALAS). Control of eALAS synthesis is a key factor in modulating heme formation by erythroid and non-erythroid cells. Much remains to be understood concerning the formation of iron centers in mitochondria and the transport of iron to the intracellular sites where non-heme iron-proteins are assembled. Recent works in yeast and humans, in relation to the disease Friedrich's ataxia, have indicated that mitochondria have a dynamic non-protein-bound, non-heme iron pool that functionally interacts with the cytosolic iron pool (Knight *et al.*, 1998). These and other works have identified components of mitochondrial iron uptake and efflux pathways (Allikmets *et al.*, 1999; Lange *et al.*, 1999).

Moreover iron is an essential cofactor for many proteins involved in normal function of neuronal tissue, such as the non-haem iron enzyme tyrosine hydroxylase, which is required for dopamine

synthesis. The oligodendrocytes use high level of iron because they are responsible for myelin production and maintenance.

In addition to controlling the flow of iron towards metabolic use, an important component of the means for establishing iron homeostasis is through alterations in iron storage capacity. Modulation of iron storage can occur through changes in synthesis and, in some cases, degradation of *ferritin*.

Recently, it has become evident that numerous cell types express the iron exporter ferroportin/Ireg1/MTP1 (McKie *et al.*, 2000; Abboud *et al.*, 2000). Recent studies on the relationship between iron and copper metabolism have shown that copper deficiency leads to an accumulation of iron in several tissues (Eisenstein, 2000). Depending on the tissue, the multicopper oxidases ceruloplasmin and hephaestin may have critical roles in iron export.

By regulating the expression of the TfR, ferritin, and the ferrous iron exporter, cells have many mechanism for preventing accumulation of excess iron.

1.7 Ferritin structure and function

Ferritin is a ubiquitous and highly conserved iron-binding protein. In vertebrates, the cytosolic form consists of 2 subunits, termed H and L. Twenty-four ferritin subunits assemble to form the apoferritin shell (fig. 5). Each apoferritin molecule of 450 KDa can sequester up to approximately 4500 iron atoms (Harrison *et al.*, 1996). Depending on the tissue type and physiologic status of the cell, ratio of H to L subunits in ferritin can vary widely, from predominantly L in such tissues as liver and spleen, to predominantly H in heart and kidney (Arosio *et al.*, 1976). The H to L ratio is not fixed, but is rather quite plastic: it is readily modified in many inflammatory and infectious conditions, and in response to xenobiotic stress, differentiation, and developmental transitions, as well as other stimuli. Ferritin H and L subunits are encoded by separate genes. Although a single functional mitochondrial ferritin gene has recently been described (Levi *et al.*, 2001). Multiple pseudogenes are also present. Ferritin also has enzymatic properties, converting Fe (II) to Fe (III) as iron is internalized and sequestered in the ferritin mineral core. Use of recombinant ferritins has demonstrated that this function is an

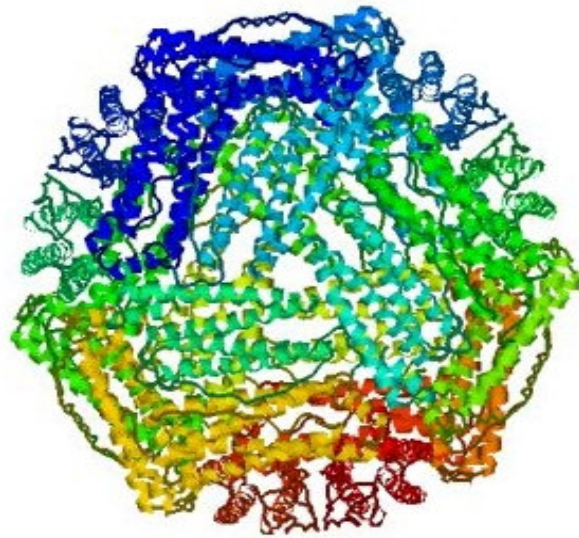


Fig. 5. Ferritin structure

Twenty-four ferritin subunits assemble to form the apoferritin shell, that has a molecular weight of ~ 450 KDa.

inherent feature of the H subunit of ferritin, which has a ferroxidase activity (Lawson *et al.*, 1989). The ferroxidase center is evolutionarily conserved, and ferroxidase activity is dramatically reduced following mutation of residues His65 and Glu62 in both human and mouse (Rucker *et al.*, 1996).

Small quantities of ferritin are present in human serum, and are elevated in conditions of iron overload and inflammation (Torti *et al.*, 1994). Serum ferritin is iron-poor, resembles ferritin L immunologically, and may contain a novel “G” (glycosylated) subunit (Santambrogio *et al.*, 1987). Despite widespread use of serum ferritin as clinical indicator of body iron stores, little is known of source of this ferritin.

The critical role of ferritin in cellular iron homeostasis is intimately linked to its primary and best-studied function of iron sequestration. The toxicity of iron in cellular systems is attributable in large part to its capacity to participate in the generation of reactive species, which can directly damage DNA, lipids, and proteins, leading to profound cellular toxicity. In the organism iron balance is maintained with exquisite care. Ferritin, by capturing and “buffering” the intracellular labile pool (Kakhlon *et al.*, 2001; Picard *et al.*, 1998) plays a key role in

maintaining iron homeostasis. It is not surprising, then, that homozygous murine knockouts of ferritin H are lethal (Ferreira *et al.*, 2000). Recently, it has become evident that regulatory factors, in addition to those that regulate iron flux, have important impact on cellular ferritin. In fact, ferritin can be viewed not only as part of a group of iron regulatory proteins that include transferrin and transferrin receptor, but also as a member of protein family that orchestrates the cellular defense against stress and inflammation (Torti *et al.*, 1988).

1.8 Ferritin in the brain

Ferritin has classically been known as an iron storage protein in many types of cells, including those of the brain. The cellular and regional distribution of ferritin in brain has been discussed (Benkovic and Connor, 1993). Recent reports have indicated the presence a ferritin receptor in the brain that is predominantly expressed in white matter (Hulet *et al.*, 1999a). This distribution indicates the presence of two, non-overlapping receptor system for iron in the brain, as transferrin receptors are mainly located in grey matter regions of the brain.

The selective expression of a ferritin receptor on the myelin producing cells, oligodendrocytes, indicates these cells have developed their own iron uptake system (Hulet et al., 2000). It is well established that iron acquisition by oligodendrocytes is essential for normal production of myelin. Hypomyelination is a consistent and predominant effect of iron deficiency in humans and animal models (Pinero and Connor, 2000) and ferritin receptor expression in myelin tracts is altered in Multiple Sclerosis (Hulet *et al.*, 1999b).

The expression of a ferritin receptor ensures that oligodendrocytes do not have to compete for Tf delivered iron in the brain and also provides these cells with the opportunity to acquire much more than could be delivered by Tf. The uptake of ferritin into oligodendrocytes is ATP and clathrin dependent (Hulet *et al.*, 2000). Alterations in ferritin levels in brain could influence iron delivery to the oligodendrocytes. Too little iron via ferritin could promote demyelination but also, elevated ferritin could be a source of iron for inducing iron mediated oxidative injury. Ferritin is present in the CSF and thus could be expected to access the interstitial fluid in the brain. The levels of CSF ferritin are roughly 10% of levels of ferritin found in the serum. Normal CSF contains approximately 3 ng/ml,

but this concentration will increase during infectious meningoencephalitis, CNS vascular diseases and dementia without vascular pathology (Sindic *et al.*, 1981). Marked elevations of CSF ferritin (30-fold) were observed in patients with bacterial or fungal meningitis in contrast to modest CSF ferritin elevations in patients with viral meningitis. Ferritin is also elevated in the cerebral spinal fluid of Multiple Sclerosis patients (Le Vine *et al.*, 1999). Consequently, CSF ferritin could be a early valuable clinical tool for differential diagnosis (Campbell *et al.*, 1986). In contrast to serum ferritin, which is highly glycosylated (>70%), ferritin within the CSF is largely non-glycosylated (<20%). Non-glycosylated ferritin is usually considered as "tissue ferritin" suggesting that CSF ferritin is derived from cell death and subsequent release (Zappone *et al.*, 1986). However, the concentration of ferritin within the CSF of normal patients is significantly higher than which would be expected to occur by passive diffusion across the blood-CSF barrier (Keir *et al.*, 1993). This suggest that local synthesis and secretion of ferritin by brain cells occurs normally.

2 . Cytoplasmatic control of ferritin synthesis

2.1 Iron-mediated regulation ferritin

Not only does ferritin sequester iron in a nontoxic form, but levels of “labile” iron regulate cellular ferritin levels, protecting cells from damage triggered by excess iron. The content of cytoplasmatic ferritin is regulated by the translation of ferritin H and L mRNAs in response to an intracellular pool of “chelatable” or “labile iron” (Konijn *et al.*, 1999). Thus, when iron levels are low, ferritin synthesis is decreased; conversely, when iron levels are high, ferritin synthesis increases. Although in certain circumstances there is an increase in ferritin mRNA in response to iron, the regulatory response of ferritin to iron is largely post-transcriptional, and due to the recruitment of stored RNA from monosomes to polysomes in the presence of iron. This process is mediated by interaction between RNA binding proteins and a sequence in the 5' untranslated region of H and L ferritin mRNA termed iron responsive element (IRE) that has a “stem-loop” secondary structure (fig. 6). There are two RNA binding proteins, iron regulatory proteins 1 and 2 (IRP1 and IRP2), that bind to this stem loop structure and inhibit RNA translation. These proteins are regulated differently: IRP1 is an iron-sulfur cluster

protein that exists in 2 forms. When iron is abundant, it exists as a cytosolic aconitase. When iron is scarce, it assumes an open configuration associated with the loss of iron atoms in the iron-sulfur cluster, and can bind the IRE stem loop, acting as a repressor of ferritin translation (fig. 7). In contrast, IRP2 is regulated by its degradation: IRP2 protein is abundant in iron insufficiency, but is degraded rapidly in iron excess through targeting of a unique 73 amino acid sequence (Iwai *et al.*, 1998) (fig. 7).

2.2 IRP1 and IRP2

The molecular cloning of IRP-1 offered insights into the structural/functional correlation that allows it to undergo changes in activity and function with no appreciable variations in protein content. In fact, this evolutionarily conserved (Andersen *et al.*, 1998) 98 kDa protein coded in human chromosome 9 (Rouault *et al.*, 1990) is highly homologous with mitochondrial (m-)aconitase, which converts citrate into isocitrate in the tricarboxylic acid cycle, with 100% identity of the amino acids involved in the formation of catalytic core (Beinert *et al.*, 1993).

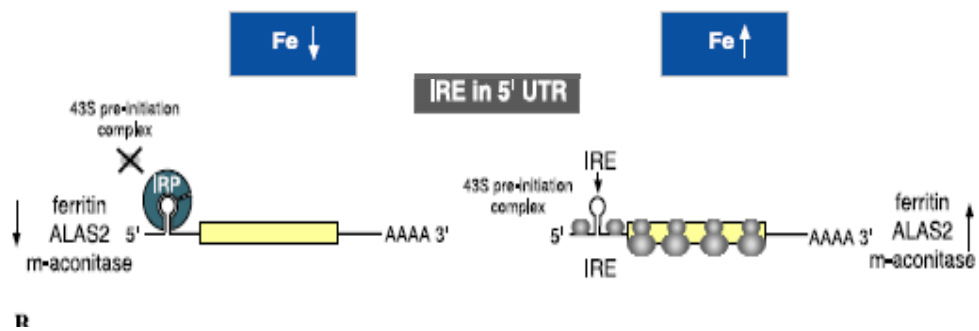
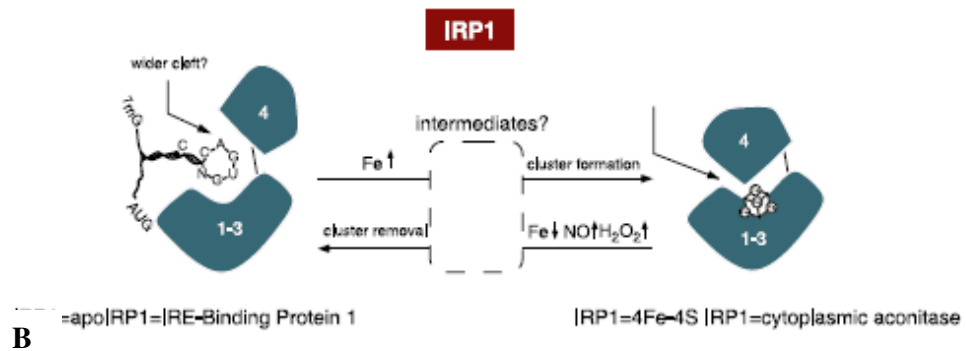


Fig. 6. Homeostatic responses to iron supply mediated by IRE-IRPs interactions.

Decreased iron supply activates binding of IRPs to IRE, resulting in translational inhibition of the mRNAs encoding ferritin (H and L chains). Conversely, IRPs do not bind to cognate IREs in iron-replete cells, permitting translation of ferritin.

A



B

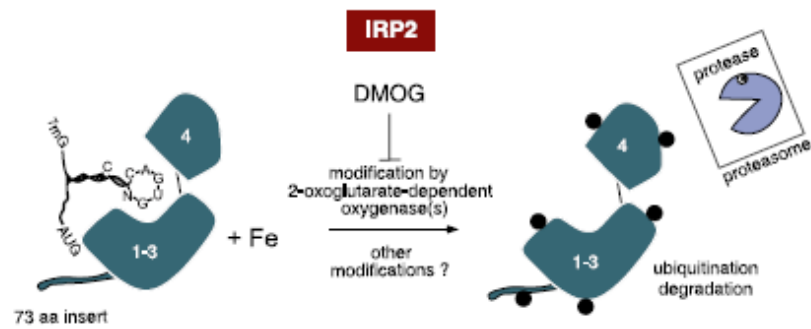


Fig. 7. IRPs regulation by iron and other stimuli

A) Post-translational regulation of bifunctional IRP1 in response to iron and other stimuli via iron-sulfur cluster switch.

B) Iron-dependent degradation of IRP2 by a mechanism involving 2-oxoglutarate-dependent oxygenases.

The abundance of information concerning the biochemistry and structure of m-aconitase has allowed the construction of an IRP-1 model that implies a post-translational switch between an apoprotein form capable of binding iron-responsive-element (IRE) motifs and an enzymically active holoprotein endowed with 4Fe-4S cluster (Eisenstein *et al.*, 1998). In the holoprotein, the four domains are in closed conformation and permit the assembly of a 4Fe-4S cubane cluster co-ordinated by cysteine residues. By contrast, as result of cluster disassembly, the apoprotein can accommodate the RNA in a cleft between domains 1-3 and 4. The switch between these two mutually exclusive functions of IRP1 is regulated by intracellular iron levels, because a high degree of aconitase activity is present under conditions of iron overload and full IRE-binding capacity exists in iron-depleted cells. The mechanism underlying the insertion and removal of cluster, and hence the conversion between the two functions of IRP1, remain poorly defined.

Although two IRE-binding proteins were initially detected by RNA bandshift assays in rat cells, IRP2 was initially detected and characterized only several years after IRP1, probably because it is

usually less abundant and can be electrophoretically distinguished from IRP1 only in murine cell extracts. IRP2 is highly homologous with IRP1, but has two major differences: the presence of a 73-amino-acid insertion in the N-terminus and lack of aconitase activity (Cairo *et al.*, 2000). The IRP2 specific sequence mediates the characteristic way by which this protein is regulated: in presence of high iron levels, IRP2 is rapidly targeted to proteasome-mediated degradation (Iwai *et al.*, 1998), and it has also been claimed that heme, rather than free iron, is involved in IRP2 degradation (Goessling *et al.*, 1998) (fig. 7). Although both IRP1 and IRP2 bind the IRE and exert an inhibitory effect on ferritin synthesis, there are evidences that IRP1 and IRP2 may have distinct tissue-specific role (Eisenstein, 2000). Thus, IRP2 knockout mice exhibit a pronounced misregulation of iron metabolism in the intestinal mucosa and central nervous system (LaVaute *et al.*, 2001). The iron overload in specific areas of the brain was associated with the development of a progressive neurodegeneration. These data establish IRP2 as an important regulator of systemic iron metabolism.

Further, relative ratios of IRP1/IRP2 differ in a tissue-specific fashion, with IRP1 being more abundant than IRP2 in liver, kidney,

intestine, and brain, and less abundant in pituitary and pro-B-lymphocytic cell line (Thomson *et al.*, 1999).

2.3 IRP regulation by stimuli other than iron

IRPs were initially appreciated as intracellular iron sensors, but it soon became clear that they also respond to other stimuli. Exposure of cells to hydrogen peroxide (H_2O_2) or nitric oxide (NO) promotes removal of IRP1 cluster and thereby induces IRE-binding activity (fig. 7). The mechanism for cluster removal is not straightforward. While the cluster of IRP1 is generally sensitive to inactivation by reactive oxygen and nitrogen species (Cairo *et al.*, 2002), which is reflected in loss of aconitase activity, this is not always associated with activation of IRE binding, which requires complete cluster disassembly. Thus, the superoxide anion ($\text{O}_2^{\cdot-}$) or peroxynitrite (NOO^{\cdot}) readily diminishes the aconitase activity of IRP1, but fails to convert it into an IRE-binding protein (Soum *et al.*, 2003). The response of IRP1 to H_2O_2 and NO are more complex. The H_2O_2 -mediated conversion of IRP1 from cytosolic aconitase to IRE-binding protein is a result of signalling pathway rather than of direct chemical modification of the 4Fe-4S cluster by H_2O_2 . First all, IRP1 activation takes place when

intact cells, but not cell extract, are exposed to H₂O₂ (Pantopoulos and Hentze; 1995). By contrast, the treatment of purified 4Fe-4S IRP1 with H₂O₂ yields 3Fe-4S IRP1, which fails to bind to IREs (Brazzolotto *et al.*, 1999). Importantly, the pathway for H₂O₂-mediated activation of IRP1 is biphasic and can only be reconstituted *in vitro* in the presence of the particulate fraction of permeabilized cells (Pantopoulos and Hentze; 1995). The latter suggests the involvement of insoluble membrane-associated factors in the pathway.

The mechanism for IRP1 activation by NO is distinct. Exposure of purified IRP1 to NO *in vitro* was recently shown to activate IRE binding (Soum *et al.*, 2003), even though in earlier literature this effect was only partial. The kinetics of IRP1 activation upon exposure of Ltk- fibroblasts to S-nitroso-N-acetyl-D,L-penicillamine (SNAP), a donor of NO, and desferrioxamine, an iron chelator, show remarkable similarities (Pantopoulos and Hentze; 1996). Thus, IRP1 activation requires at least 4h of continuous treatment with these drugs, while the “stress activation” of IRP1 is triggered by a transient pulse with H₂O₂ and occurs within 30-60 min. Moreover, SNAP and desferrioxamine also elicit the activation of IRP2, which does not

contain an aconitase-type cluster. These findings are compatible with model, according to which NO may modulate the LIP and thereby promote responses to iron deficiency. It is also conceivable that a direct, NO-mediated cluster destabilization of IRP1 also accounts at least for a partial activation of IRE binding *in vivo*.

3. Hypoxia

Hypoxia is oxygen starving at the tissue and cellular levels. It is caused by reduction of oxygen supply in blood physiological levels. Severe hypoxia can result in anoxia, a complete loss of oxygen to an area of tissue. There are four major types of hypoxia. The first type, hypoxic hypoxia, is decrease of fraction of inhaled oxygen possibly due to hyperventilation from respiratory depression or altitude above sea level. The second type of hypoxia is termed anaemic hypoxia, and is characterized by a decrease in the amount of haemoglobin that binds oxygen in the blood. This can be caused by multiple factors, including but not limited to: blood loss, reduced red blood cell production, carbon monoxide poisoning, and a genetic defect of haemoglobin. Stagnant hypoxia, the third type of hypoxia that has been defined, results in low blood flow and is caused by

vasoconstriction and/or heart failure. The fourth type of hypoxia is hystotoxic hypoxia, a poisoning of oxidative enzymes that causes vasodilatation in brain arteries and veins, resulting in more blood flow to the brain tissues. This response is probably mediated by nitric oxide (NO) and adenosine. Hypoxia is a fundamental angiogenic stimulus. An important mediator of this primary stimulus is hypoxia-inducible TOR-1 α (HIF-1 α) (Wang *et al*, 1995). Normally, this protein is oxidized, ubiquitinated and degraded in the proteasome. In the absence of oxygen, HIF-1 α levels increase and stimulate VEGF transcription. Cells of the innate immune and in tissues below system get energy almost entirely from glycolysis, enabling survival under a variety of harsh conditions. In a recent report HIF-1 α is now placed at the center of metabolic control in these cells (Cramer *et al.*, 2003). The regulation of most proteins required for hypoxic adaptation occurs at the gene level and involves transcriptional induction via the binding of a transcription factor, hypoxia-inducible factor-1 (HIF-1), to the conserved sequence, 5-(A/T)CGTG-3, in the hypoxia response element (HRE) on the regulated genes (Semenza *et al.*, 1997). To date, about 100 hypoxia-inducible genes have been found to be directly regulated by HIF-1.

HIF-1 is a heterodimer composed of 120 kDa HIF-1 α subunit and a 91-94 kDa HIF-1 β subunit, both of which are members of basic helix-loop-helix (bHLH)-PAS family. PAS is an acronym for the three members first recognised (Per, ARNT, and Sim). According, HIF-1 α and HIF-1 β each contain a bHLH domain near the N-terminus preceding the PAS domain. Whereas the basic domain is essential for DNA binding, the HLH domain and N-terminal half of the PAS domain are necessary for heterodimerization and DNA binding. Moreover, there are two transcriptional activation domains (TADs) in HIF-1 α , the N-terminal activation domain (TAD-N), and the C-terminal activation domain (TAD-C). In contrast, HIF-1 β contains only one transcriptional activation domain at C-terminus. Furthermore, HIF-1 α possess a unique oxygen-dependent degradation domain (ODD) that controls protein stability. In addition to the ubiquitous HIF-1 α , the HIF-1 α family contains two other members, HIF-2 α (also called EPAS, MOPS or HLF) (Tian *et al.*, 1997; Hogenesch *et al.*, 1997; Ema *et al.*, 1997) and HIF-3 α (Gu *et al.*, 1998), both of which have more restricted tissue expression (Wenger *et al.*, 2002). HIF-2 α and HIF-3 α contain domains similar to those in HIF-1 α and exhibit similar biochemical properties, such as heterodimerization with HIF-1 β and DNA binding to the

same DNA sequence *in vitro*. HIF-2 α is also tightly regulated by oxygen tension and its complex with HIF-1 β appears to be directly involved in hypoxic gene regulation, as is HIF-1 α (Wiesener *et al.*, 1998). However, although HIF-3 α is homologous to HIF-1 α , it might be a negative regulator of hypoxia-inducible gene expression (Hara *et al.*, 2001). To active transcription, HIF-1 α must recruit the transcriptional adapter/histone acetyltransferase proteins, p300 and CBP to the target gene promoters. This occurs by direct physical interactions between the transactivation domain (TAD) of HIF-1 α and the first cysteine-histidine (CH1) domain of the p300/CBP complex. This domain of p300/CBP also binds member of the CITED (CBP /p300 interacting transactivator with ED-rich tail) family of transcription factors. CITED2 and CITED4 disrupt the interaction between HIF-1 α and p300 and inhibit transactivation by HIF-1 α and gene activation by hypoxia.

3.1 Regulation of HIF-1

3.1.1 Oxygen-dependent

At normal oxygen levels, HIF-1 prolyl-hydroxylases hydroxylate the prolyl residues at Pro 402 and 564 of the HIF-1 α ODD. Furthermore, the asparagine hydroxylase FIH-1 (factor inhibiting HIF-1) hydroxylates Asp 803 of the HIF-1 α C-terminal transactivation domain. The hydroxylated peptide interacts with an E3 ubiquitin-protein ligase complex. After being poly-ubiquitinated, HIF-1 α is degraded by the 26S proteasome. Under hypoxic conditions, HIF-1 α is not hydroxylated because the major substrate, dioxygen, is not available. The unmodified protein escapes the VHL-binding, ubiquitination and degradation, and then dimerizes with HIF-1 β . The heterodimeric HIFs upregulate a myriad of hypoxia-inducible genes, triggering physiologic responses to hypoxia. Interestingly, PHD-1 and -2 are inducible by hypoxia, indicating a feedback loop to avoid nuclear HIF-1 accumulation.

3.1.2 Oxygen-independent

In addition to mediating adaptation to hypoxia, HIF-1 also contributes to other cellular processes that occur under normoxic conditions, such as the development of normal tissues or tumors, the determination of cell death or survival, immune responses and the adaptation to mechanical stress. Under normoxic conditions HIF-1 can be activated by various cytokines, growth factors, transition metals, iron chelation (inhibits enzymatic activity), as well as nitric oxide (NO). Degradation of HIF-1 in a VHL- and oxygen-independent manner is mediated by p53. Dephosphorylated HIF1 α binds to p53 while phosphorylated HIF-1 α is the major form that binds to HIF-1 β (Fox *et al.*, 2004). HIF-1 α protects p53 degradation by binding to Mdm2, the principal cellular antagonist of p53 (Chen *et al.*, 2003). Also, inhibition of PI3K or mTOR prevent growth factor- and cytokine-induced HIF-1 α accumulation. Generally HIF-1 α induction by hypoxia is far greater than by growth factors and cytokines. The COP9 subunit CSN5 is able to stabilize HIF-1 α in a pVHL-independent form aerobically by inhibiting HIF-1 α prolyl-564 hydroxylation (Bemis *et al.*, 2004).

3.2 Hypoxia-mediated iron regulation

The link between hypoxia and iron has strengthened with the evidence of hypoxic regulation of proteins that regulate iron homeostasis. Indeed, all the major genes of iron metabolism respond to hypoxia. First, it has been shown that hypoxia or CoCl_2 (which mimics hypoxia), results in a three-fold increase in TfR RNA, despite a decrease of IRP1 activity (Tacchini *et al.*, 1999). Demonstration of a HIF-1 binding site in the TfR promoter suggests that the observed increase in TfR RNA results from hypoxia-induced stabilization of HIF-1 and increased transcription of the TfR gene rather than a change in TfR mRNA stability (Tacchini *et al.*, 1999). Second, serum transferrin (Tf) levels increase in animals exposed to hypoxia (Simpson *et al.*, 1996) and hypoxia increases Tf gene expression in hepatoma cells (Rolfs *et al.*, 1997). Tf is also a member of the HIF-1-regulated gene family (Bolann and Ulvik, 1987) (fig. 8). Finally, as noted above, the activities of the RNA-binding proteins, IRP-1 and

IRP-2 are also regulated by hypoxia. Hypoxia exposure decreases IRP1-RNA binding activity and increases IRP2-RNA binding activity. The hypoxic increase in IRP2-RNA binding results from increased IRP2 protein levels (Hanson *et al.*, 1999). Hypoxia stabilizes the [4Fe-4S] active form of IRP1 at the expense of its RNA-binding activity (Hanson and Leibold, 1998). Indeed, it appears that, IRP2 plays a more critical role than IRP1 (Hanson *et al.*, 1999).

3.3 Ferritin regulation during hypoxia-ischemia

Tissue ischemia and cellular hypoxia have been studied in a number of conditions and changes in ferritin documented. Hypoxia in neonatal rat oligodendrocytes and human oligodendrogliomas induced the synthesis of ferritin. This effect was not inhibited by actinomycin D, nor did RNA levels of ferritin H RNA change. The effects on ferritin in oligodendrocytes was recapitulated by exogenous iron and blocked by desferrioxamine (Qi *et al.*, 1995). Similar effects on ferritin induction were observed in a rat model of acute hypoxic/ischemic insult. Shortly, after the hypoxic-ischemic

insult, ferritin-positive microglia accumulate in subcortical white matter. In addition, the ratio of H to L ferritins shifts toward H-rich ferritins, especially in the hemisphere in which both hypoxic and ischemic insult was applied (Cheepsunthorn *et al.*, 2001). In another ischemic-reperfusion model of the rat brain, induction of both ferritin H and L mRNAs occurred in the ischemic insult hemisphere. Protein levels, determined by immunohistochemistry, parallely rises in mRNA; surprisingly, although overall induction of H and L mRNA was equal, the distribution of H and L ferritin RNA as determined by in situ hybridization of rat brains was completely different (Chi *et al.*, 2000). Ferritin changes in hypoxia are at least in part mediated by altered regulation of the IRP proteins. IRP1 binding activity decreased under hypoxic conditions in rat hepatoma cells (Hanson and Leibold, 1998); IRP1 decreased and ferritin levels increased in hypoxic mouse macrophages (Kuriyama *et al.*, 2001). In contrast, IRP2 activity was found to increase under similar conditions (Toth *et al.*, 1999). The period of reperfusion after ischemia is thought to be a critical period during which oxidant damage is maximal in many tissues, including heart, brain, and other organs. During post-ischemic reoxygenation of rat liver, early ferritin degradation was counteracted by enhanced ferritin transcription and concomitant IRP

down-regulation. It was suggested that this might act to re-establish ferritin levels and limit reperfusion damage (Tacchini *et al.*, 1997). Similarly, in a model of transient surgically-induced segmental intestinal ischemia/reperfusion in rats, cytosolic ferritin RNA and protein decreased after 3 and 6 hours of reperfusion. By 12 hours, ferritin mRNA but not protein had increased to higher than normal levels. Ferritin appeared to be regulated both pre-translationally and translationally in response to ischemia reperfusion (Yeh *et al.*, 1998). Consistent with these findings, reoxygenation was found to induce IRP1 in a hepatoma cell line (Hanson and Leibold, 1998) (fig. 8).

3.4 How would hypoxia regulate iron metabolism?

One proposed mechanism of hypoxic regulation of iron metabolism is via hydrogen peroxide (H_2O_2), possibly from a heme-containing oxygen sensor that acts as an IRP2 degradation signal (Hanson *et al.*, 1999). A decrease in peroxide output from such a sensor during hypoxia would thus act to stabilize IRP2. The use of oxygen-derived free radicals in the regulation responses appears to be a general mechanism for regulating the stability of proteins that mediate hypoxic adaptation.

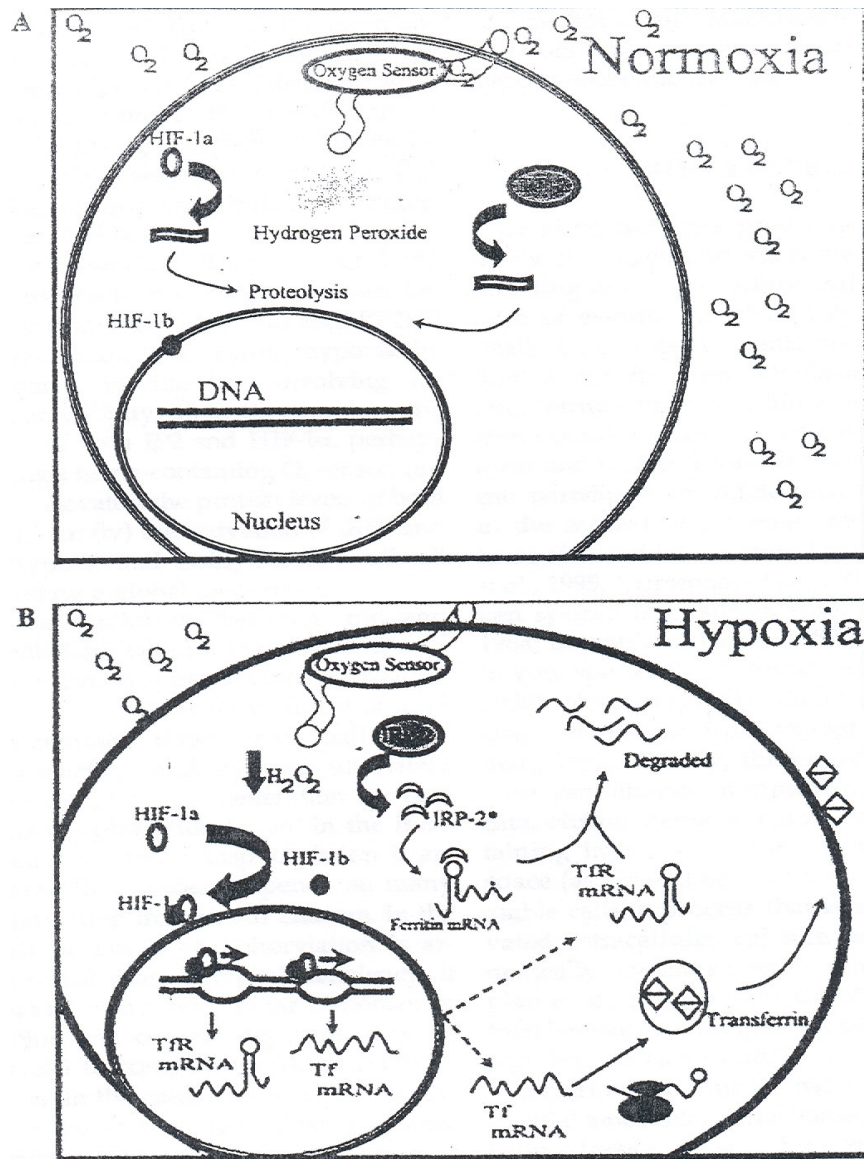


Fig. 8. Hypoxia and iron metabolism

A. Normoxic Cell. This cell is well oxygenated, and the oxygen sensor is saturated. This may lead to generation of H_2O_2 , which is known to facilitate degradation of HIF-1 α and IRP-2.

B. Hypoxic Cell. This cell is hypoxic is signalled by the oxygen sensor, again possibly by a decrease in H_2O_2 concentration. HIF-1 α is stabilized and after heterodimerizing with HIF-1 β , HIF-1 translocates into the nucleus, where it binds to the hypoxia response element (HRE) upstream of a multitude of genes, including TfR and Tf. IRP2 is also stabilized and activated.

For example, hypoxia-induced stabilization of HIF- 1 α protein is blocked in the presence of H₂O₂ (Fandrey *et al.*, 1994), suggesting that hypoxia-induced changes in the level of this reactive oxygen species may involved in HIF-1 activation (Hanson *et al.*, 1999). HIF- 1 α subunits are targeted for rapid degradation in normoxic cells by a proteosomal mechanism operating on an internal oxygen-dependent degradation domain (ODD) (Huang *et al.*, 1998). Under hypoxic conditions, IRP2 stability would depend on the relative cytosolic concentrations of the Fe²⁺ and H₂O₂. The Fe²⁺ concentration may be high enough to inactivate the RNA binding activity of IRP1 and convert it to its aconitase form, but because of the simultaneous decrease in H₂O₂, the concentration may not be sufficient to signal the degradation of IRP2. Data suggest that pVHL might be required for oxygen-dependent HIF 1 degradation. The ability of pVHL to degrade HIF1 appears to be iron-dependent. Treatment with iron chelators prevented the association of pVHL with HIF1, suggesting that iron may be necessary for the interaction of pVHL with HIF1 (Maxwell *et al.*, 1999). Leibold and co-workers (Hanson *et al.*, 1999) have suggested four analogies between hypoxic regulation of HIF-1 α and IRP2: i) Both proteins accumulate during hypoxia by post-translational mechanisms involving increased protein stability; ii)

CoCl₂ stimulates the accumulation of both IRP2 and HIF-1 α , perhaps by inactivating a heme-containing O₂ sensor; iii) iron chelator elevated the protein levels of both IRP2 and HIF- 1 α ; iiiii) the activation of IRP2 and HIF- 1 α by hypoxia and CoCl₂ occurs in all cell types, suggesting a global mechanism.

Clearly, the similarities between iron and oxygen metabolism suggest that iron and oxygen regulate overlapping cellular activities. Both iron depletion and hypoxia ultimately compromise cellular ATP generation by curtailing oxidative phosphorylation. In the iron-depleted cell, oxidative phosphorylation is arrested because this process depends on many enzymes containing iron-sulfur clusters. In the hypoxic cell oxidative phosphorylation is arrested due to substrate (oxygen) deficiency. It appears that the common cellular responses to iron depletion and oxygen depletion may be ways for cell to compensate for its ATP-deprived status. In iron depletion, the cell compensates in two ways. First, to restore the free iron available for essential cellular processes, the cell tries to increase its iron uptake and decrease its iron storage. Second, while the intracellular iron is being replenished, the cell tries to find other means of generating ATP. To this end, iron-depleted cells upregulate glycolytic

enzymes and glucose transporters via a HIF1-dependent pathway. Similarly, in the case of hypoxia, the cell compensates for ATP-depletion by increasing glycolysis. Here, the hypoxic stimulus causes the stabilization of HIF-1 α , ultimately resulting in transcriptional up-regulation of glycolytic enzymes and glucose transporters. Augmenting ATP generation may be one important mechanism by which iron chelators could prevent neuronal injury during hypoxic-ischemic insults.

4. MATERIALS AND METHODS

4.1 Animals

Female Wistar rats (Charles River, Calco, Lecco, Italy) were housed in diurnal lighting conditions (12 h darkness and 12 h light) and fasted overnight but allowed free access to water before the experiment. Experiments were performed according to international guidelines for animal research and the experimental protocol was approved by the Animal Care Committee of the University of Naples “Federico II”.

4.2 Primary cortical neuronal cultures

Cortical neurons were obtained from brains of 15–16-day-old Wistar rat embryos (Scorziello *et al.*, 2001). Briefly, the rats were anesthetized and then decapitated to minimize the animals' pain and distress. Dissection and dissociation were performed in Ca²⁺/Mg²⁺-free phosphate buffered saline (PBS) containing glucose (30 mM). Tissues were incubated with papain for 10 min at 37°C and dissociated by trituration in Earle's balanced salt solution (EBSS) containing DNase, bovine serum albumin (BSA) and ovomucoid. Cells were plated at a concentration of 15×10⁶ on 100-mm plastic

Petri dishes precoated with poly-D-lysine (20 µg/mL) in Ham's F12 nutrient mixture/Eagle's minimal essential medium containing glucose (1:1), supplemented with 5% of deactivated fetal calf serum (FCS) and 5% of deactivated horse serum (HS), L-glutamine (2 mM) and penicillin (50 units/mL) and streptomycin (50 µg/mL). Cytosine arabinoside (arabioside-C) (10 µM) was added within 48 h of plating to prevent the growth of non-neuronal cells. Neurons were cultured at 37°C in a humidified 5% CO₂ atmosphere with medium replenishment after 6 days, and used after 11 days of culture in all experiments.

4.3 Primary glial cell cultures

Cultures of cortical type-1 astrocytes were obtained as described elsewhere (McCarthy and de Vellis, 1980). In brief, 2-3-day-old Wistar rats were decapitated, the brains were removed under aseptic conditions and placed in PBS containing 100 units/mL penicillin and 100 µg/mL of streptomycin. Under a stereomicroscope, cortices were dissected, the meninges were carefully removed, and the tissues were cut into small fragments, digested with trypsin at 37°C for 20 min., and mechanically dissociated in Dulbecco's modified Eagle's medium (DMEM) containing 100 units/mL of penicillin and 100

$\mu\text{g}/\text{mL}$ of streptomycin, 10% FCS and 2 mM glutamine. The medium was changed after 24 h and then twice a week. Once confluent, the cultures were shaken vigorously to remove non-adherent cells and sub-cultured 1:3. The cells were then mechanically purified and sub cultured once again 1:4 before the experiments were performed. This protocol produced cultures in which 95% of cells were positive to glial fibrillary acid protein.

4.4 Glioma cells

Rat glioma cells (C6 line) were grown in DMEM containing 4.5 g/L glucose and supplemented with 10% fetal bovine serum (FBS), L-glutamine (2 mM), penicillin (100 units/mL) and streptomycin (100 $\mu\text{g}/\text{mL}$). For iron repletion-depletion experiments, cells were treated with 50 $\mu\text{g}/\text{mL}$ ferric ammonium citrate (FAC) as a source of Fe ions or with 100 μM desferrioxamine (Desferal, Novartis, Origgio, Varese, Italy) for 18 h.

4.5 Combined oxygen and glucose deprivation and reoxygenation

Cortical neurons, type-1 astrocytes and C6 glioma cells were exposed to oxygen and glucose deprivation (OGD) for various times according to a previously reported protocol (Goldberg and Choi,

1993). Briefly, the culture medium was replaced with deoxygenated (saturated for 20 min. with 95% N₂ and 5% CO₂), glucose-free Earle's balanced salt solution containing NaCl 116 mM, KCl 5.4 mM, MgSO₄ 0.8 mM, NaHCO₃ 26.2 mM, NaH₂PO₄ 1 mM, CaCl₂ 1.8 mM, glycine 0.01 mM and 0.001 w/v phenol red. Cultures were then placed in an humidified 37°C incubator within an anaerobic chamber (Billups-Rothenberg, Inc., Del Mar, CA) containing a gas mixture of 95% N₂ and 5% CO₂. The final oxygen concentration in the medium in these experimental conditions, measured by oxygen-sensitive electrode (OxyLite 2000, Oxford Optronix, Oxford, UK), was 5 mm Hg. Reoxygenation (Reoxy) was achieved by replacing the OGD medium with oxygenated regular medium containing glucose and returning cultures to normoxic conditions (37°C in a humidified 5% CO₂ atmosphere) for various times.

4.6 Permanent middle cerebral artery occlusion (pMCAO) and identification of the ischemic area.

The pMCAO procedure is described elsewhere (Tortiglione *et al.*, 2002). Briefly, animals were anesthetized intraperitoneally with chloral hydrate (400 mg/kg). The left temporoparietal region of the head was shaved and a 2 cm incision was made vertically between

the orbit and the ear. Under an operating stereomicroscope (Nikon SMZ800, Florence, Italy), an incision was made dividing the temporal muscle, and the left lateral aspect of the skull was then exposed by reflecting the temporal muscle surrounding soft tissue. An opening (diameter =2 mm) was made with a high-speed microdrill through the outer surface of the semitranslucent skull, just over the visibly identified middle cerebral artery. A saline solution was applied to the area to prevent heat injury. Using a pair of fine forceps, the inner layer of the skull was removed and the dura and arachnoid were opened. The pMCAO was achieved by electrocoagulation with a bipolar electrocauterizer (Diatermo MB122, G.I.M.A., Milan, Italy) without damaging the brain surface.

At various times after pMCAO, animals were decapitated and the brains removed. Sham-operated controls underwent surgical procedures except for the electrocoagulation of the middle cerebral artery. The brain was placed on dry-ice and the coronal sections were cut with a vibratome (Campden Instrument, 752M, London, UK) beginning at 1 mm posterior to the anterior pole. Coronal slices 0.5- and 2-mm thick were alternately cut. The 0.5-mm slices, stained in 2% triphenyltetrazolium chloride-saline solution, were used to identify the ischemic core. The 2-mm slices were used to dissect the

ischemic core, identified by triphenyltetrazolium chloride in the previous adjacent slice, and the non-ischemic surrounding area. The contralateral hemisphere was processed in the same manner. After surgical removal, the samples were immediately frozen in liquid nitrogen and kept at -80°C until analysis.

4.7 Preparation of cytosolic and mitochondrial extracts

After OGD and OGD/Reoxy exposure cortical neurons, type-1 astrocytes and C6 glioma cells were washed and scraped off with PBS containing 1 mM EDTA. To obtain cytosolic extracts for electrophoretic mobility shift assay (EMSA) and ferritin Western blot analysis, cells were treated with lysis buffer containing 10 mM HEPES, pH 7.5, 3 mM MgCl_2 , 40 mM KCl, 5% (v/v) glycerol, 1 mM dithiothreitol (DTT), 0.2% (v/v) Nonidet P-40 (NP-40) and protease inhibitor tablet (Roche, Mannheim, Germany) at 4°C . Cell debris and nuclei were pelleted by centrifugation at 15,000 g for 10 min. at 4°C and supernatants were stored at -80°C . For Western blot analysis of cytochrome c and caspase-3, cells were collected by scraping and low-speed centrifugation. Cell pellets were lysed at 4°C for 1 h in a buffer containing 10 mM KCl, 1.5 mM MgCl_2 , 20 mM HEPES, pH 7.5, 1 mM EGTA, 1 mM EDTA, 1 mM DTT, 0.1 mM

phenylmethylsulphonyl fluoride and proteases inhibitors tablets (Roche). The mitochondrial-containing fraction was obtained by centrifugation at 16,000 g for 25 min. Cytosolic extracts mitochondria-free were obtained by centrifugation of supernatants at 100,000 g for 30 min. in a Beckman L8-70 ultracentrifuge. The protein concentration was determined by the Bio-Rad protein assay according to the supplier's manual (Bio-Rad, Milan, Italy).

4.8 Electrophoretic mobility-shift assay (EMSA)

Plasmid pSPT-fer, containing the sequence corresponding to the IRE of the H-chain of human ferritin, linearized at the *Bam* HI site, was transcribed *in vitro* with T7 RNA polymerase (Promega). The transcriptional reaction was performed at 38.5 °C for 1 h with 200 ng of plasmid in the presence of 50 µCi of [α -³²P] CTP (800 Ci/mM) (Amersham Biosciences) and 0.5 mM ATP, GTP and UTP (Promega), in 20 µl reaction volume (Festa *et al.*, 2000a). The DNA template was digested with 10 units of RNase-free DNase I for 10 min at 37 °C. Free nucleotides were removed on Sephadex G-50 column (Boehringer- Mannheim). For RNA-protein band-shift analysis, cytosolic extracts (5 µg) were incubated for 30 min. at room temperature with 0.2 ng of *in-vitro* transcribed ³²P-labeled IRE RNA.

The reaction was performed in buffer containing 10 mM HEPES, pH 7.5, 3 mM MgCl₂, 40 mM KCl, 5% (v/v) glycerol, 1 mM DTT and 0.07% (v/v) NP-40, in a final volume of 20 µL. To recover total IRP1 binding activity, cytosolic extracts were pre-incubated for 10 min with 2-mercaptoethanol at a 2% (v/v) final concentration, before the addition of ³²P-labeled IRE RNA. IRP2 activity was differentiated by super-shift assay incubating cytosolic extracts with a goat polyclonal anti-IRP2 antibody (Santa Cruz Biotechnology Inc, Santa Cruz, CA) for 45 min. at room temperature before electrophoresis. Unbound RNA was digested for 10 min. with 1 unit of RNase T₁ (Roche) and non specific RNA-protein interactions were displaced by the addition of 5 mg/mL heparin for 10 min. RNA-protein complexes were separated on 6% non denaturing polyacrylamide gel for 2 h at 200 V. After electrophoresis, the gel was dried and autoradiographed at -80°C. The IRP-IRE complexes were quantified with a GS-700 imaging densitometer and/or with a GS-505 molecular imager system (Bio-Rad). The results are expressed as the percentage of IRP binding activity versus 2-mercaptoethanol-treated samples.

4.9 Western blot analysis

Samples containing 50 µg of proteins were denatured, separated on a 12% (for ferritin) or 15% (for cytochrome c and caspase-3) SDS-polyacrylamide gel and electro-transferred onto a nitrocellulose membrane (Amersham Biosciences, Little Chalfont, Buckinghamshire, UK) using a Bio-Rad Transblot. Proteins were visualized on the filters by reversible staining with Ponceau-S solution (Sigma) and destained in PBS. Membranes were blocked at 4°C in milk buffer (1X PBS, 10% (w/v) non fat dry milk, 0.1 % (v/v) Triton X-100) and then incubated for 3 h at room temperature with 1:250 sheep polyclonal antibody to human ferritin (Bioscience International, Saco, Maine), 1:1000 mouse monoclonal anti-cytochrome c antibody (Bioscience International, Camarillo, CA) or 1:1500 rabbit polyclonal anti-caspase-3/ CPP32 antibody (Transduction Laboratories, Lexington, KY). Subsequently, the membranes were incubated for 90 min. at room temperature with donkey peroxidase-conjugated anti-sheep IgG for ferritin determination (Bioscience International) and with sheep peroxidase-conjugated anti-mouse and anti-rabbit IgG for cytochrome c and caspase-3/ CPP32 determination (Amersham Biosciences). The

resulting complexes were visualized using chemoluminescence Western blotting detection reagents (ECL, Supersignal West Pico, Pierce, Rockford, IL). The optical density of the bands was determined by a GS-700 imaging densitometer and/or a gel image analysis system (Chemi Doc Imaging System, Bio-Rad). Normalization of results was ensured by incubating the nitrocellulose membrane in parallel with the β -actin antibody.

4.10 Metabolic labeling with ^{35}S -methionine/cysteine and immunoprecipitation

Cells were pre-incubated for 30 min. at 37°C in a methionine-cysteine-free medium. The medium was removed and the cells were labeled with 80 $\mu\text{Ci}/\text{mL}$ Promix L- ^{35}S -label (Amersham Biosciences) in the appropriate methionine-cysteine-free medium for 3 h during normoxic, OGD or OGD/reoxygenation conditions. Cells were washed three times with PBS and lysed in buffer containing 50 mM Tris-HCl, pH 7.5, 150 mM NaCl, 1% (v/v) Triton X-100 and protease inhibitor tablet (Roche). Aliquots of cytosolic lysates from neurons containing 500 μg of proteins or from C6 cells and from cortical type-1 astrocytes containing 850 μg of proteins were cleared with protein G PLUS-Agarose (Santa Cruz). Then 5 μg of anti-ferritin

antibody, previously conjugated with 30 μ L of protein G PLUS-Agarose, were added to the lysates and incubated overnight at 4°C. The protein-agarose beads were pelleted, washed three times with cold lysis buffer and boiled with SDS loading buffer. Immunoprecipitated proteins were resolved by using 12% SDS-PAGE. After electrophoresis the gel was treated with Amplify (Amersham Biosciences) for 30 min., fixed, dried and then visualized by autoradiography. Normalization of the incorporation of 35 S-methionine/cysteine into total proteins was made by measuring trichloroacetic precipitable radioactive counts or protein content.

4.11 RNA extraction and Northern blot analysis

After OGD and OGD/Reoxy treatments, total cellular RNA was isolated from cells by the TRIzol reagent (Invitrogen Life Technologies, Carlsbad, CA) extraction method. The TRIzol reagent is a ready-to-use for the isolation of total RNA from cells. The reagent, a mono-phasic solution of phenol and guanidine isothiocyanate, is an improvement to the single step RNA isolation method developed by Chomczynski (Chomczynski *et al.*, 1987). Briefly, cells grown in monolayer were lysed directly in culture dish by adding 1 mL of TRIzol reagent to a 3.5 cm diameter dish, and

passing the cell lysate several times through a pipette. The amount of TRIzol reagent was based on the area of the culture dish (1 mL per cm²). The homogenized samples were incubated in tube for 5 min at room temperature to permit the complete dissociation of nucleoprotein complexes. 200 μ L of chloroform were added to each sample and tubes were shaken vigorously for 15 seconds and then incubated for 3 min at room temperature. Successively, samples were centrifuged at 12,000 \times g for 15 min at 4°C. Following centrifugation, the mixture separates into a lower red, phenol-chloroform phase, an interphase, and a colorless upper aqueous phase. RNA remains exclusively in the aqueous phase (about 60% of the volume of TRIzol reagent used). The aqueous phase was transferred to a fresh tube and RNA was precipitated by mixing with 500 μ L of isopropyl alcohol. After centrifugation at 12,000 \times g at 4°C for 15 min, RNA precipitate forms a gel-like pellet on the side and bottom of the tube.

For Northern blots 10 μ g of total RNA were fractionated on a 1.5% agarose denaturing formaldehyde gel in MOPS buffer. RNA was transferred by blotting in 20X SSC (1X SSC, 0.15 M NaCl, 0.015 M Na-citrate) , pH 7.0, to Hybond-N filters (Amersham Biosciences). The hybridization was performed for 18 h at 65°C in 0.5 M sodium phosphate buffer, pH 7.2, 1 mM EDTA, pH 8.0, 7% (w/v) SDS. The

filters were washed in 0.05 M sodium phosphate buffer pH 7.2, 1% (w/v) SDS at 65°C and autoradiographed at -80 °C. A cDNA fragment corresponding to human cDNA for H-ferritin was ³²P-radiolabelled using the random priming method (TaKaRa Biomedicals, Otsu, Shiga, Japan). 100 ng of template DNA and 2 µL of random primer were combined in a microcentrifuge tube, and sterile distilled water was added to a final volume of 14 µL. The mix was heated at 95°C for 3 min and then cooled on ice for 5 min. Then 2.5 µL of 10 X buffer, 2.5 µL of the dNTP mixture and 5 µL (50 µCi) of ³²P-labelled dATP ([α-³²P] dATP, 3000 Ci/mM, Amersham Biosciences) were added to the mixture. Successively, 1 µL of Exo-free Klenow fragment was added (total final volume 25 µL) and the mix was incubated at 37°C for 1 h. The polymerase reaction was stopped by adding 0.5 µL EDTA 0.5 M and probes were purified on a Bio-Spin 30 chromatography column (Bio-Rad). The β-actin probe was used to standardize the amounts of mRNA in each lane.

4.12 Cell viability assay

Cell viability was assessed by measuring the level of mitochondrial dehydrogenase activity using 3-(4,5-dimethyl-2-thiazolyl)-2,5-

diphenyl-2H-tetrazolium bromide (MTT) as substrate (Hansen *et al.*, 1989). The assay was based on the redox ability of living mitochondria to convert dissolved MTT into insoluble formazan. Briefly, after OGD and OGD/Reoxy, the medium was removed and the cells were incubated in 1 mL of MTT solution (0.5 mg/mL) for 1 h in a humidified 5% CO₂ incubator at 37°C. The incubation was stopped by removing the MTT solution and adding 1 mL of DMSO to solubilize the formazan. The absorbance was monitored at 540 nm by using a Perkin-Elmer LS 55 Luminescence Spectrometer (Perkin-Elmer Ltd, Beaconsfield, UK). The data are expressed as the percentage of cell viability to control cultures.

4.13 Lipid peroxidation assay

Lipid peroxidation products from cells were measured by the thiobarbituric acid colorimetric assay (Esterbauer and Cheeseman, 1990). Briefly, after OGD and OGD/Reoxy cells were washed and collected in PBS Ca²⁺/Mg²⁺ free medium containing 1 mM EDTA and 1.13 mM butylated hydroxytoluene (BHT). Cells were broken up by means of sonicator. Trichloroacetic acid, 10% (w/v), was added to cellular lysate and, after centrifugation at 1,000 g for 10 min., the supernatant was collected and incubated with 0.5 % (w/v)

thiobarbituric acid at 80°C for 30 min. After cooling, malondialdehyde (MDA) formation was recorded (A_{530} nm and A_{550} nm) in a Perkin Elmer LS-55 spectrofluorimeter. Samples were scaled for protein concentration determined by the Bio-Rad protein assay and a standard curve of MDA was used to quantify the MDA levels formed during the experiments. The results are presented as percentage of MDA production versus a control obtained in untreated cultures.

4.14 Apoferritin treatment of cortical neurons

Primary cortical neurons, cultured in Ham's F12 nutrient mixture/Eagle's minimal essential medium as above described, were treated for 18 h with 0.3 mg/mL apoferritin (Sigma-Aldrich, St Louis, MO) that is easily pinocytosed by the cell (Balla *et al.*, 1992; Festa *et al.*, 2000b). After treatment cells were washed, culture medium was replaced with deoxygenated glucose-free Earle's balanced salt solution, and then were exposed to OGD and OGD/reoxygenation. Lipid peroxidation products from cells were measured as above described. The intracellular ferritin content in cytosolic extract was determined using a fluorimetric enzyme immunoassay system according to the supplier's manual (Enzymum test, Roche). The results are expressed as ng of ferritin/mg of cell protein.

4.15 Statistical analysis

The densitometric data of EMSA, Western blot, Northern blot, biosynthesis bands and neurons apoferritin treatment are reported as means \pm SEM. Statistical significance among the means was determined by the ANOVA followed by the Newman-Keuls test. A p value ≤ 0.05 was considered statistically significant.

5. RESULTS

5.1 IRP RNA-binding activity in cortical neurons and in glial cells after OGD

To determine the effects of OGD on IRP RNA-binding activity, we exposed cortical neurons from rat embryos, primary cultures of rat astrocytes type-1 and C6 rat glioma cells to normoxic and hypoxic conditions for 0 to 5 h and then we measured the IRP RNA-binding activity by RNA band-shift assay. As shown in Fig. 9 in cortical neurons, OGD significantly enhanced IRP1 RNA-binding activity. This effect appeared after only 30 min. of OGD exposure (22% increase vs control), peaked at 3 h (98% of increase vs control) and persisted up to 5 and 12 h (data not shown). To determine the total amount of IRP1 RNA-binding activity, β -mercaptoethanol was added to the binding reactions before the addition of ^{32}P -labeled IRE probe. β -mercaptoethanol reveals "latent" IRP1 RNA-binding activity thus giving the total amount (100% of IRE-binding) of IRP1 activity (Hentze *et al.*, 1989). Addition of β -mercaptoethanol to neuron extracts did not enhance further OGD-stimulated IRP1 RNA-binding activity (Fig. 9A, lanes 6-10), suggesting that OGD promoted

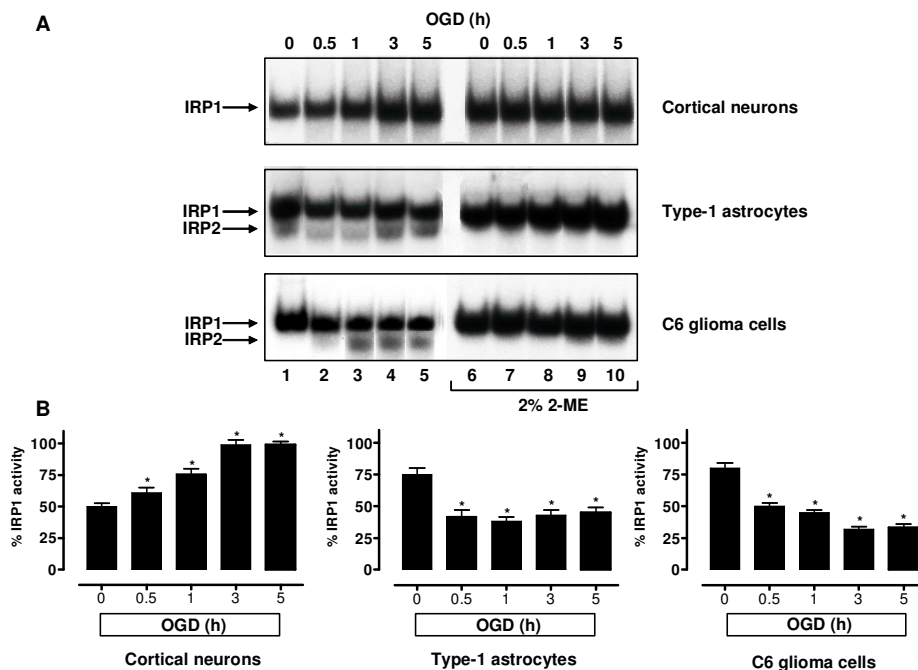


Fig. 9. IRP1 and IRP2 RNA-binding activity in rat cerebral cells during OGD

(A) RNA band-shift assay performed in the absence (lanes 1-5) or presence (lanes 6-10) of 2% β -mercaptoethanol (2-ME). Cortical neurons, astrocytes and C6 glioma cells were grown under normoxic conditions (lane 1) or hypoxic conditions (lanes 2-5). RNA-protein complexes were separated on non-denaturing 6% polyacrylamide gels and revealed by autoradiography. (B) IRP1-RNA complexes were quantified by densitometric and/or PhosphorImager analysis. The results of lanes 1-5 were plotted as percent of respective controls treated with 2-ME. Lane 6 of each panel represents 100% of IRP1 RNA-binding activity. * $p < 0.05$ compared with controls.

maximal IRP1-RNA association without altering the IRP1 protein content.

Differently, type-1 primary astrocytes responded to OGD with a decrease (42% decrease vs control) in IRP1 RNA-binding activity after 30 min. and this reduction persisted up to 5 h. Addition of β -mercaptoethanol determined an increase in IRP1 RNA-binding activity in all samples (Fig. 9 A, lanes 6-10), suggesting that the OGD-induced inactivation of IRP1 was not due to a variation in IRP1 protein levels nor to modifications that irreversibly inactivated IRP1 RNA-binding.

Exposure of C6 glioma cells to OGD produced a similar rapid decrease (38% decrease vs control) of IRP1 RNA-binding after 30 min., reaching a maximum decrease of 60% vs control at 3 h. This reduction also persisted for 5 h. Concomitant to the IRP1 RNA-binding decrease, there was a slight OGD-dependent increase in IRP2 RNA-binding activity. It should be noted that 2-mercaptoethanol treatment decreases IRP2 activity in both glial cells. This phenomenon could be explained by the sensibility of IRP2 to redox influence. In fact, routine *in vitro* treatment of cell extracts with 2% 2-mercaptoethanol, useful to maximally activate IRP1 binding

activity, results in underestimation of IRP2 activity (Bouton *et al.*, 1997).

5.2 Response of IRP2 to iron concentration during OGD

To verify that the faster migrating band was IRP2, we treated C6 cells for 18 h with 50 µg/mL iron salt ferric ammonium citrate (FAC) or with 100 µM of the potent iron chelator desferrioxamine (DFX), and then exposed the cells to OGD. Under normoxic conditions the IRP2-IRE complex was not present in either the control or iron-treated cells but appeared in iron-depleted cells (Fig. 10, lanes 1–3). This is in accordance with iron regulation of IRP2 (Iwai *et al.*, 1998). In cells exposed to OGD, the faster migrating band disappeared upon exposure to FAC (lane 5) and reappeared upon exposure to DFX (lane 6), indicating that this band corresponded to the IRP2-IRE complex. These results were confirmed by super-shift assay using IRP2-specific antibody (Fig. 10, right side).

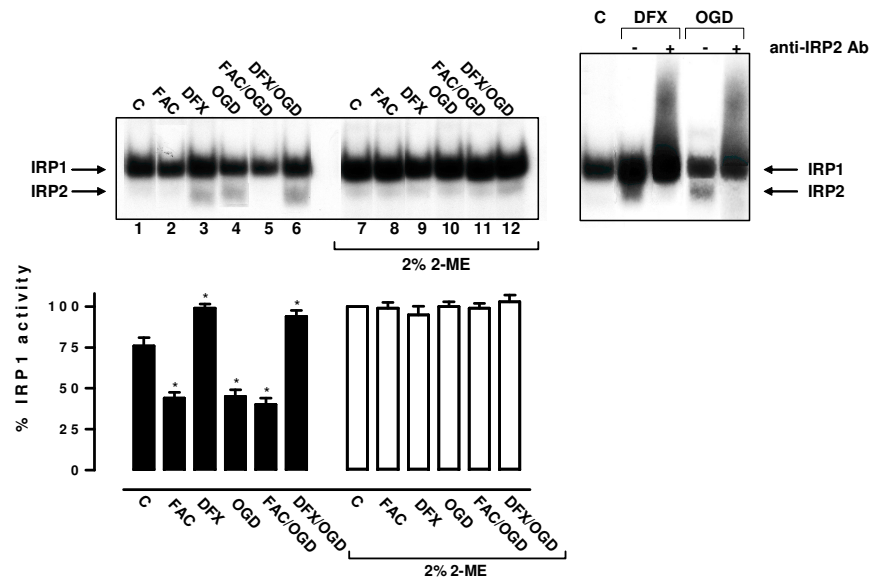


Fig. 10. Response of IRPs to intracellular iron concentration during OGD
 Rat glioma C6 cells were exposed to ferric ammonium citrate (FAC) for 18 h, desferrioxamine (DFX) for 18 h, OGD for 3 h. Cytosolic extracts from cells exposed to normoxic conditions (lanes 1-3) or to 3 h of OGD (lanes 4-6) were subjected to RNA band-shift assay. Experiments were performed in the absence (lanes 1-6) or presence (lanes 7-12) of 2% β -mercaptoethanol (2-ME). IRP2 activity was also identified by super-shift assay using a goat polyclonal anti-IRP2 antibody (right side).

5.3 IRP RNA-binding activity during OGD followed by reoxygenation

It has been reported that the reoxygenation reverts the hypoxic modulation of IRP RNA-binding activity in several cell types (Tacchini *et al.*, 1997; Hanson and Leibold, 1998; Schneider and Leibold, 2003). To test whether reoxygenation reverted IRP modulation by OGD also in cortical neurons and glial cells, cells were exposed to OGD for 3 h and reoxygenated for 3 and 24 h after which IRP RNA-binding activity was measured and results are depicted in Fig. 11. In cortical neurons, reoxygenation gradually reverted OGD-induced IRP1 activation, and baseline levels were reached within 24 h of treatment. On the contrary, in C6 glioma cells IRP1-RNA binding activity increased after 3 h of reoxygenation, and reached control level after 24 h. IRP2 RNA-binding became undetectable after 24 h of reoxygenation, as occurred in cells cultured in normoxic conditions. Similarly, in astrocytes IRP1 RNA-binding activity was completely restored after 24 h of reoxygenation, although there was no significant variation after 3 h of reoxygenation.

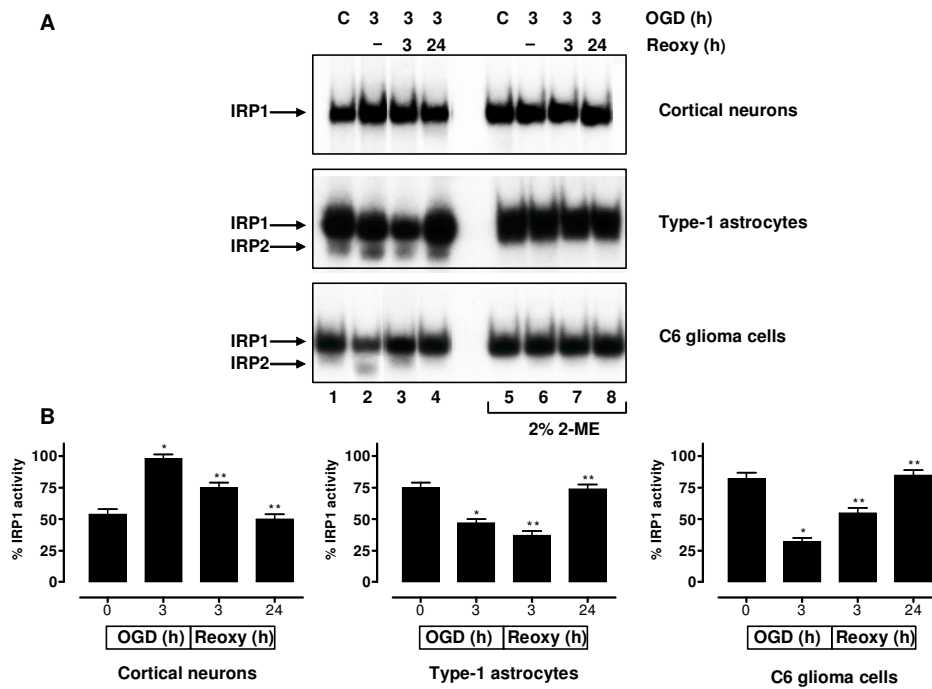


Fig. 11. IRP1 and IRP2 RNA-binding activity in rat cerebral cells during reoxygenation

(A) Cortical neurons, astrocytes and C6 rat glioma cells were exposed for 3 h to OGD (lane 2 of the respective panels) followed by re-exposure to normoxia (Reoxy), for 3 and 24 h (lanes 3 and 4). Cytosolic extracts were incubated with an excess of ^{32}P -labeled IRE probe in the absence (lanes 1–4) or presence (lanes 5–8) of 2% β -mercaptoethanol (2-ME). (B) IRP1-RNA complexes were quantified by densitometric and/or PhosphorImager analysis and the results plotted as percent of controls treated with 2-ME (lane 5 of each panel, which corresponds to 100% of IRP1 RNA-binding activity). * $p < 0.05$ compared with control; ** $p < 0.05$ compared with 3 h of OGD.

5.4 Effects of OGD and OGD/reoxygenation on ferritin expression

To evaluate the combined effect of OGD and following reoxygenation on ferritin expression in cortical neuronal and glial cells, we determined ferritin protein levels by Western blot analysis after 3 h of OGD and after OGD followed by 3 and 24 h of reoxygenation. In cortical neurons ferritin content resulted unchanged after 3 h of OGD and after 3 h of reoxygenation, while there was a significant 1.6-fold increase in the late phase of reoxygenation (24 h) (Fig. 12). On the contrary, after 3 h of OGD ferritin levels significantly increased by about 2.0- and 1.8-fold in astrocytes and C6 glioma cells, respectively. In C6 cells the exposure to reoxygenation for 3 h determined a decrease in ferritin content, which however was higher than control. After 24 h of reoxygenation, ferritin amount decreased to baseline levels. Similarly, in astrocytes ferritin content decreased during reoxygenation (33% decrease vs OGD after 24 h reoxygenation).

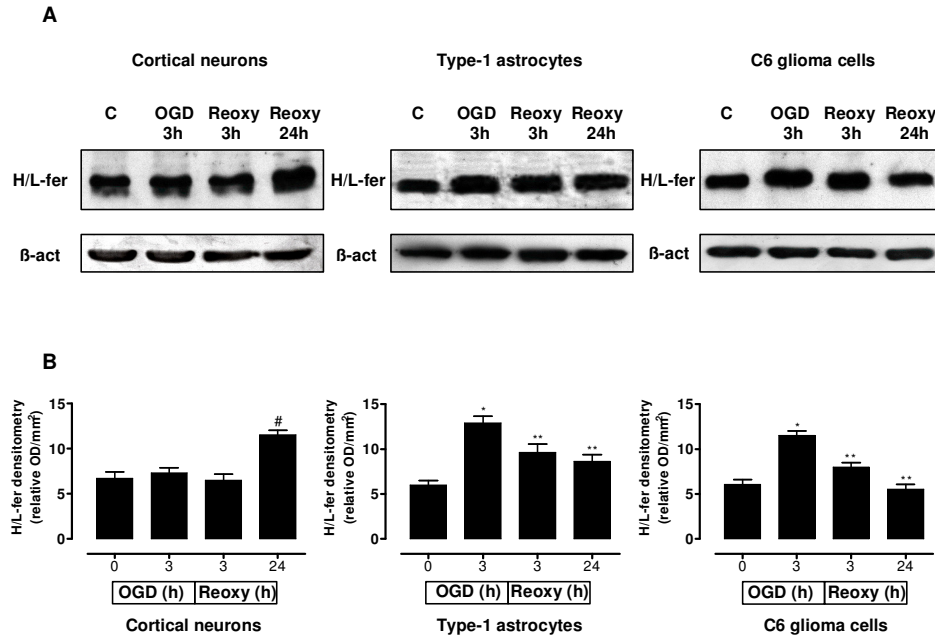


Fig. 12. Effects of OGD and OGD/Reoxy on cellular ferritin levels

(A) Rat cortical neurons, type-1 astrocytes and C6 glioma cells were exposed for 3 h to OGD followed by re-exposure to normoxia for 3 and 24 h (Reoxy). Equal amounts of cytosolic lysates of proteins were fractionated by 12% SDS-PAGE and subjected to Western blot analysis (B) The bands corresponding to ferritin were quantified by densitometric analysis and plotted as arbitrary units. The anti- β -actin antibody was used to standardize the amounts of proteins in each lane. # $p < 0.05$ as compared to other experimental groups; * $p < 0.05$ as compared to control group; ** $p < 0.05$ as compared to 3 h of OGD.

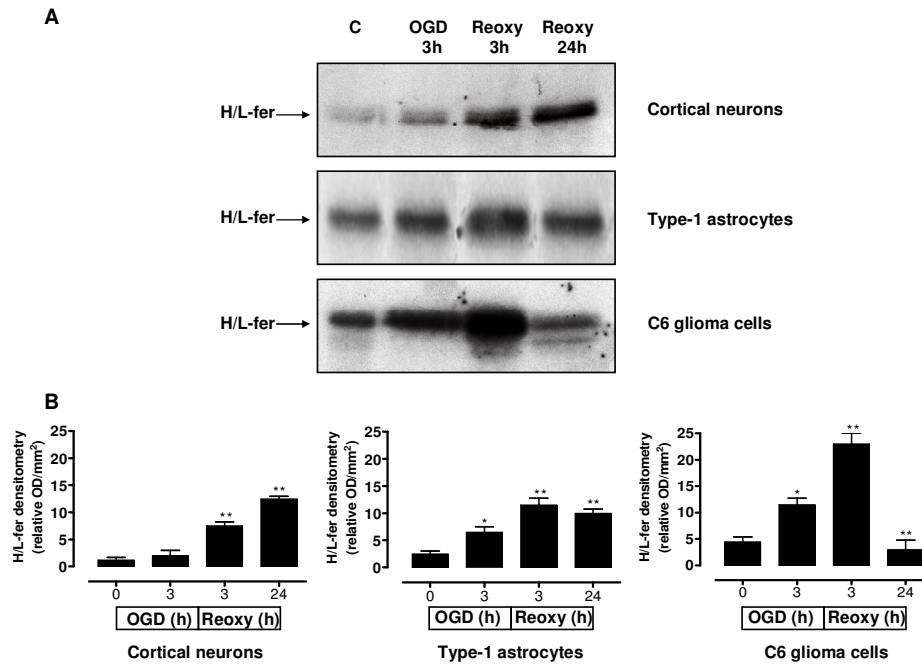


Fig. 13. Ferritin synthesis during OGD and OGD/Reoxy

(A) Cortical neurons, astrocytes and C6 glioma cells were exposed to OGD (3 h) followed by reoxygenation (Reoxy) for 3 and 24 h. Cells were labeled with ³⁵S-Met/Cys. Cell extracts were immunoprecipitated and proteins subjected to SDS-PAGE analysis and autoradiography. (B) The bands corresponding to ferritin were quantified by densitometric analysis and plotted as arbitrary units. * $p < 0.05$ compared with control; ** $p < 0.05$ compared with 3 hr of OGD.

5.5 Effects of OGD and OGD/reoxygenation on ferritin biosynthesis

We evaluated ferritin biosynthesis by immunoprecipitation of ³⁵S-labelling in cortical neurons, type-1 astrocytes and C6 cells exposed to OGD and OGD/reoxygenation (Fig. 13). In type-1 astrocytes the rate of ³⁵S-methionine/cysteine incorporation into ferritin enhanced of about 2.6-fold during the OGD and progressively increased of about 4.6-fold during the subsequent reoxygenation phases. In C6 cells ferritin biosynthesis was increased of about 2.6-fold during 3 h of OGD. The subsequent 3 h of reoxygenation increased ferritin biosynthesis by about 5-fold, and after 24 h of reoxygenation ferritin returned to control levels. Similar experiments with cortical neurons showed a consistent increase in ferritin biosynthesis only during the reoxygenation phase, i.e., a 6- and 11-times increase after 3 and 24 h, respectively.

5.6 Analysis of H-ferritin mRNA levels after OGD and OGD/reoxygenation

To assess whether the improved ferritin level observed during OGD and OGD/reoxygenation might result from transcriptional control, we analyzed by Northern blot the steady-state levels of H-ferritin

mRNA (Fig. 14). In type-1 astrocytes the level of H-ferritin mRNA resulted slightly decreased after the OGD exposure and progressively increased during the reoxygenation phases (3 and 24 h). Instead H-ferritin mRNA content remained unchanged in C6 cells exposed to OGD and OGD/reoxygenation. Differently, in cortical neurons Northern blot analysis showed a significant increase of H-ferritin mRNA amount (about 2.3-fold) only in the late phase of reoxygenation (24 h).

5.7 Effects of OGD and OGD/reoxygenation on lipid peroxidation and on cell survival

To investigate the effects of OGD and OGD/reoxygenation on cell survival, we evaluated cell viability by MTT assay, cell membrane injury by MDA production, and the induction of apoptotic features by cytochrome c release and activated caspase-3 expression evaluation. Exposure of cortical neurons to OGD for 3 h induced impairment of mitochondrial oxidative capacity (fig. 15) associated with increased MDA production (fig.16). When the neurons were exposed to OGD/reoxygenation, an enhanced mitochondrial activity impairment was associated with a significant increase of lipid peroxidation.

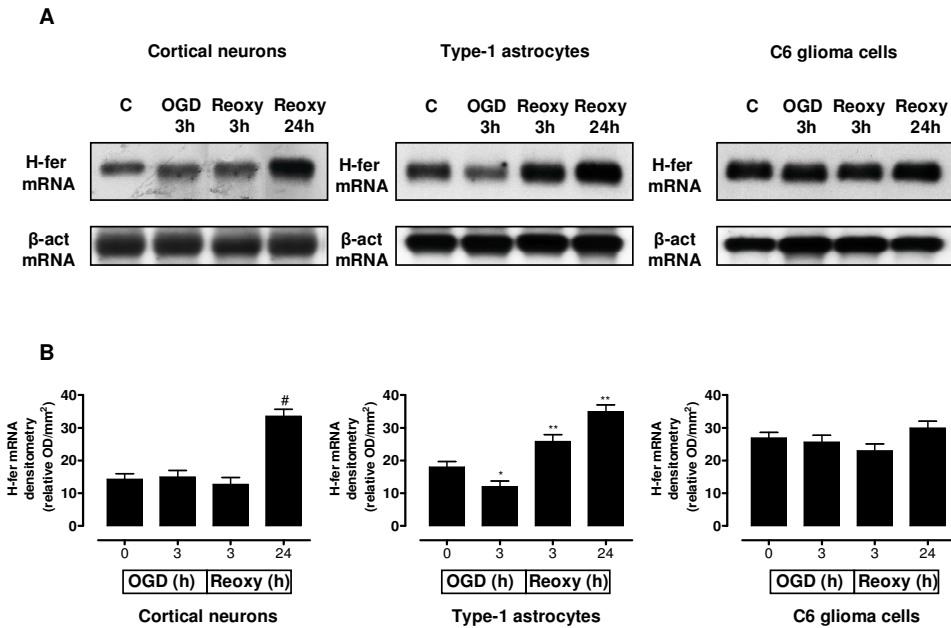


Fig. 14. Northern blot analysis for H-ferritin mRNA levels

A) RNA was isolated from cortical neurons, astrocytes and C6 glioma cells exposed for 3 h to OGD followed by reoxygenation for 3 and 24 h (Reoxy). 10 μ g of total cellular RNA were hybridized to H-ferritin cDNA ³²P-radiolabeled probe. The β -actin probe was used to standardize the amounts of mRNA in each lane. (B) The bands corresponding to H-ferritin mRNA were quantified by densitometric and/or PhosphorImager analysis and plotted as arbitrary units. # $p < 0.05$ as compared to other experimental groups; * $p < 0.05$ as compared to control group; ** $p < 0.05$ as compared to 3 h of OGD.

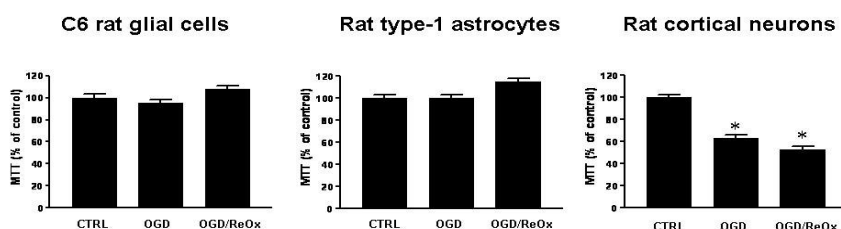


Fig. 15. Effects of OGD and OGD/reoxygenation on survival of cortical neurons and glial cells.

Primary cultures of cortical neurons were exposed to OGD (3 hrs) and to OGD/reoxygenation (24 hrs). Cell viability was assessed by measuring the level of mitochondrial dehydrogenase activity using 3-(4,5-dimethyl-2-thiazolyl)-2,5-diphenyl-2H-tetrazolium bromide (MTT) as substrate. The data are presented as percentage of insoluble formazan production versus a control obtained in untreated cultures (left side). * $p < 0.05$ compared with untreated cultures.

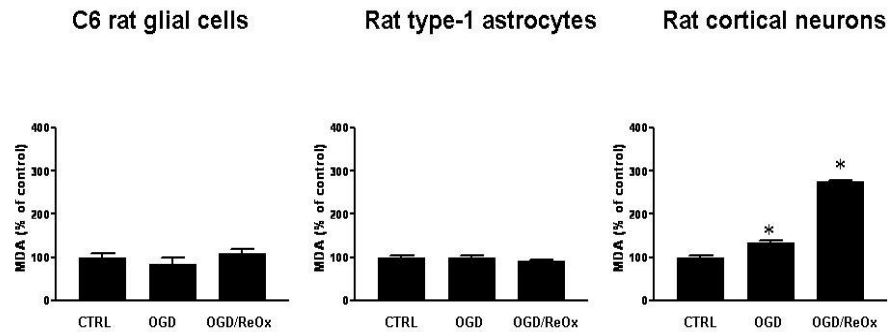


Fig.16. Effects of OGD and OGD/reoxygenation on free radical production in cortical neurons and glial cells.

Primary cultures of cortical neurons and glial cells were exposed OGD and OGD/reoxygenation (24 h). Lipid peroxidation was measured by a thiobarbituric acid colorimetric assay and the data are presented as percentage of MDA production versus a control obtained in untreated cultures. * $p < 0.05$ compared with untreated cultures.

Exposure of cortical neurons to OGD and to subsequent reoxygenation caused the release of cytochrome c into cytosol and induced activation of caspase-3, two hallmarks of apoptosis. Conversely, OGD and OGD/reoxygenation did not significantly modify mitochondrial oxidative capacity or MDA production in either astrocytes or glioma cells. No apoptotic features were identified in either cell type. In Fig. 17 are showed the results of Western blot analysis for cytochrome c release and caspase-3 cleavage in all cell types analysed. The results are summarized in Table 1.

5.8 Effect of exogenous ferritin addition on lipid peroxidation in cortical neurons exposed to OGD followed by reoxygenation

To establish whether the greater vulnerability observed in cortical neurons compared to glial cells was related to the delayed increase in ferritin biosynthesis occurring during the OGD/reoxygenation phase, we exposed cortical neurons to apoferritin which is easily pinocytosed by the cell (Balla *et al.*, 1992; Festa *et al.*, 2000b) via receptors that have been identified in the CNS (Hulet *et al.*, 2000). Then we evaluated ferritin effect on OGD/reoxygenation-induced lipid peroxidation. To this aim cortical neurons were pretreated with

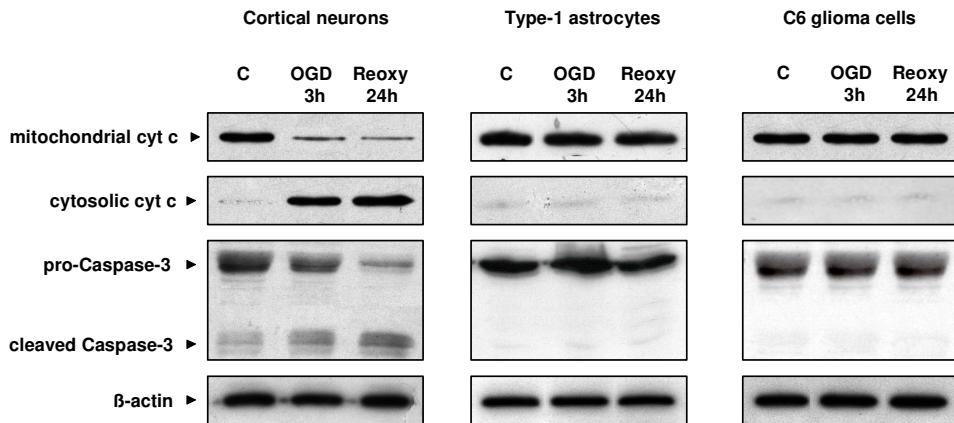


Fig. 17. Western blot analysis for cytochrome c release and for pro-caspase-3 cleavage

Cortical neurons, astrocytes and C6 glioma cells were exposed for 3 h to OGD followed by reoxygenation for 24 h (Reoxy). Equal amounts of proteins from cytosolic and mitochondrial fractions were electrophoresed on 12% SDS-PAGE and subjected to Western blot analysis using cytochrome c and caspase-3/ CPP32 antisera. Immunocomplexes were detected by chemoluminescence. Caspase-3/ CPP32 antibody recognizes both the 32 kDa unprocessed pro-caspase-3 and the 17 kDa subunit of active caspase-3. The anti-β-actin antibody was used to standardize the amounts of proteins in each lane.

Table 1. Effect of OGD and OGD/Reoxygenation on cellular survival and lipid peroxidation					
Type of rat cells	Treatment	MTT assay ^a %	MDA production %	Cyt. c release	Caspase-3 cleavage (CPP32)
Cortical neurons	Control cells	100±3.9	100±7.6	no release	no cleavage
	OGD 3h	63±4.8 *	133±8.7 *	release	cleavage
	OGD 3h/ Reoxy 24h	53±4.8 **	275±7.1 **	release	cleavage
Type-1 astrocytes	Control cells	100±10	100±10	no release	no cleavage
	OGD 3h	100±10	100±10	no release	no cleavage
	OGD 3h/ Reoxy 24h	115±10	91±10	no release	no cleavage
C6 glioma cells	Control cells	100±6.9	100±14	no release	no cleavage
	OGD 3h	95±5.8	83±28.9	no release	no cleavage
	OGD 3h/ Reoxy 24h	108±4.8	108±19.6	no release	no cleavage
^a MTT assay was performed in normoxic condition for 1h after OGD exposure * P<0.05 v.s Control; ** P<0.05 v.s. OGD					

Table 1. Effects of OGD and OGD/reoxygenation on free radical production and on survival of cortical neurons and glial cells.

apoferritin (0.3 mg/mL) for 18 h, exposed to OGD and OGD/reoxygenation. Ferritin concentration was determined in cytosolic extracts by enzyme immunoassay system and the results showed an increased ferritin content in neurons after apoferritin treatment compared to control cells (Fig. 18). Preincubation of neurons with exogenous apoferritin reduced the lipid peroxidation occurring after the OGD/reoxygenation phase of 57% (Fig. 18), thus suggesting that the increased intracellular content of the iron-scavenging ferritin is indeed related to antioxidant cellular defense.

5.9 In vivo cerebral ischemia modulates IRP-RNA binding and affects ferritin levels

To investigate *in vivo* the molecular mechanisms governing changes in ferritin levels during hypoxia, we used the pMCAO procedure as a model of cerebral ischemia. Protein extracts of ischemic core and the area surrounding the ischemic core after 3, 6, 9 and 24 hr of pMCAO were processed for IRP RNA-binding activity analysis. As shown in Fig. 19 A IRP1 activity resulted increased in the ischemic core after 3 hr of pMCAO and progressively decreased reaching the

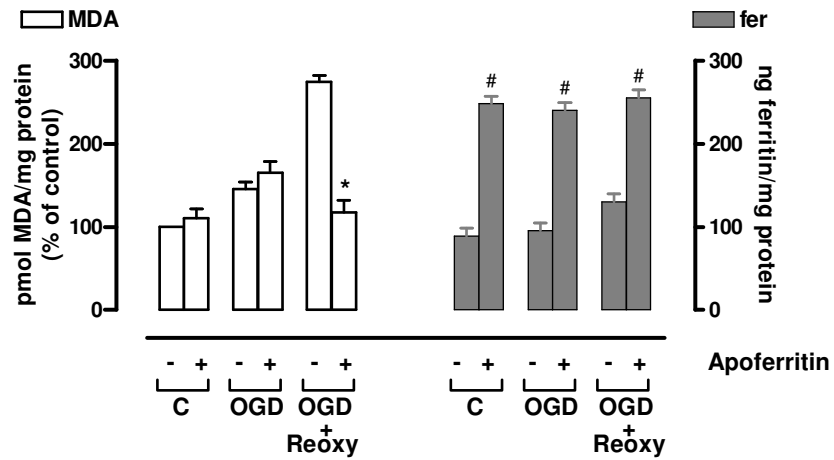


Fig. 16. Ferritin effect on lipid peroxidation in cortical neurons exposed to OGD followed by reoxygenation

Cortical neurons were incubated with apoferritin (Apo) for 18 h before exposure to OGD (3 h) and then exposed to reoxygenation (24 h). Cells were lysed, lipid peroxidation was evaluated and the data are presented as percentage of MDA production versus untreated cultures (left side). * $p < 0.05$ compared with untreated neurons exposed to OGD/reoxygenation. Ferritin concentration was determined by the enzyme immunoassay system (right side). # $p < 0.05$ versus respective controls.

baseline levels at 24 hr. On the contrary, IRP1 binding activity was unchanged in protein extracts of the area surrounding the ischemic core. Addition of β -mercaptoethanol resulted in similar IRP1-binding activity in all samples, suggesting that ischemia-mediated changes in IRP1 in the brain occurred without changes in IRP1 protein level. Ferritin content, evaluated by Western blot, decreased in the ischemic core after 24 hr of pMCAO as compared to the contralateral area (Fig. 19 B). No changes in ferritin levels were found in the extract from the area surrounding the ischemic core.

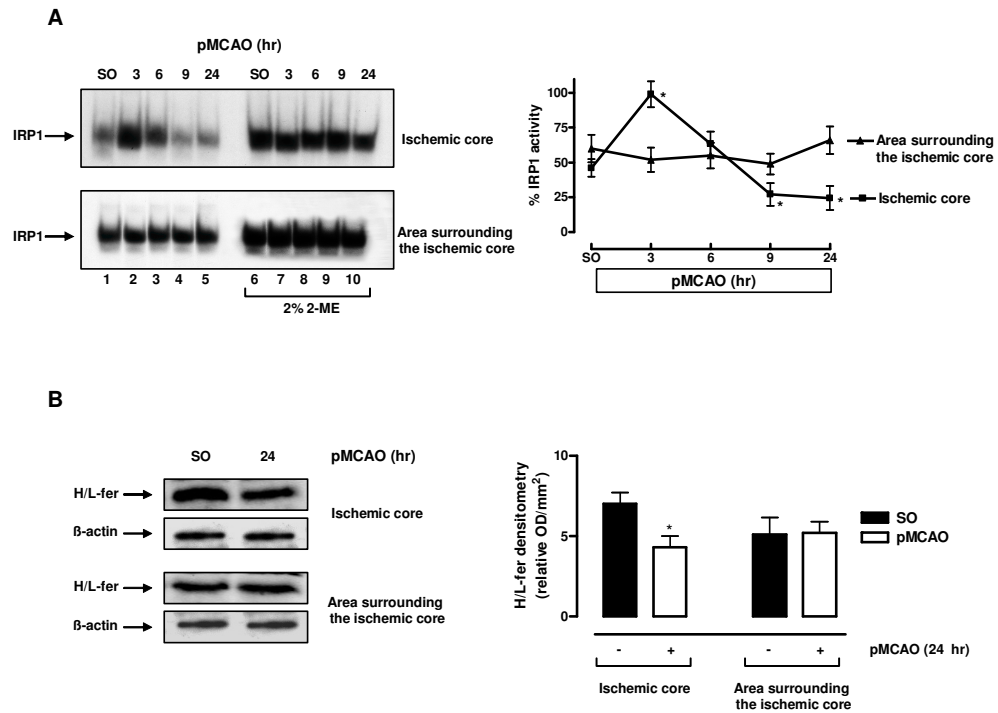


Fig. 19. Effects of *in vivo* cerebral ischemia on IRPs RNA-binding and ferritin levels

(A) Proteic extracts from ischemic core and penumbra regions of rat brain exposed to pMCAO were subjected to RNA band-shift assay using an excess of ^{32}P -labeled IRE probe in presence (lanes 6-10) or absence (lanes 1-5) of 2% β -mercaptoethanol (2-ME). (B) Equal amounts of proteins from ischemic and penumbra rat brain regions were fractionated by 12% SDS-PAGE and subjected to Western blot analysis. Ferritin was visualized by chemoluminescence Western blotting detection reagents.

6. DISCUSSION AND CONCLUSIONS

Perturbations in cellular iron and ferritin are emerging as an important element in the pathogenesis of disease. These changes in ferritin are important not only in the classic diseases of iron acquisition, transport and storage, such as primary hemochromatosis, but also in diseases characterized by inflammation, infection, injury, and repair. Among these are some of the most common diseases that afflict mankind: neurodegenerative diseases such as Parkinson disease (Linert *et al*, 2000) and Alzheimer disease (Kondo *et al*, 1996), vascular diseases such as cardiac and neuronal ischemia-reperfusion injury (Chi SI *et al*, 2000) and a variety of premalignant conditions and cancers .

We demonstrated that oxygen-glucose deprivation followed by reoxygenation affects IRP1 activity and ferritin biosynthesis differently in cortical neurons and glial cells (Irace *et al.*, 2005) IRP1 binding activity was significantly decreased in primary cultures of type-1 astrocytes and C6 glioma cells during OGD. On the contrary, OGD remarkably increased IRP1 binding activity in primary cultures of cortical neurons. The experiments with the reducing agent 2-mercaptoethanol, which maximally activates "latent" IRP1 RNA-

binding activity, show that the effects were not caused by a change in IRP1 protein content during OGD. The evidence that hypoxia did not affect IRP1 protein content coincides with data obtained in human embryonic kidney cells (Hanson *et al.*, 1999). In addition, IRP2 binding activity occurred in astrocytes and, at a higher level, in C6 glioma cells exposed to OGD, but not in cortical neurons. The presence of IRP2 in glia-derived cells could be due to the differential expression of IRP2 in different cerebral cell types (Leibold *et al.*, 2001) or to the developmental status of the cells (Siddappa *et al.*, 2002). Moreover, in glial cells OGD had an opposite effect on the IRPs, i.e. it decreased IRP1 binding activity and increased IRP2 binding activity. The same divergent modulation occurs in epithelial HEK293 cells (Hanson *et al.*, 1999; Schneider and Leibold, 2003) and in some mammalian tissues (Meyoron-Holtz *et al.*, 2004). The increase of IRP2 binding activity during OGD could be due to the accumulation of IRP2 protein (Hanson *et al.*, 1999; Schneider and Leibold, 2003) as a consequence of an oxygen-dependent decrease in IRP2 ubiquitination (Hanson *et al.*, 2003). Thus, it appears that oxygen tension exerts a relevant, opposite role in the modulation of IRP1 and IRP2 binding activity, even if can not be excluded that IRPs may

themselves be subjected to not yet identified regulatory mechanisms induced by OGD/reoxygenation.

In C6 glioma cells, intracellular iron can also contribute to IRP1 and IRP2 hypoxia-induced regulation. It is generally agreed that iron overload and iron depletion exert a regulatory function through IRP1 [4Fe-4S] cluster assembly/disassembly and IRP2 degradation/stability (Pantopoulos, 2004). Interestingly, our results in glioma cells show that, when the increase or decrease of iron levels inhibit or stimulate IRP1 and IRP2 activity, respectively, the subsequent reduction of oxygen tension by OGD did not further affect IRP binding activity. This is compatible with the hypothesis that iron and oxygen regulate the Fe-S aconitase/IRP1 cluster switch from the same site.

During reoxygenation, the OGD-induced changes in IRPs binding activity were reverted and progressively returned to normoxic levels in neuronal and glial cells. Restoration of IRPs activity by normoxic conditions agrees with reports on non-excitabile cells (Tacchini *et al.* 1997, 2002; Hanson and Leibold, 1998; Schneider and Leibold, 2003). The results obtained during reoxygenation can be ascribed to restoration of oxygen level or to production of radical oxygen species (ROS) that elicit activation of IRP1 (Hanson and Leibold, 1998).

During OGD and reoxygenation phase, the opposite and differential modulation of IRPs occurring in neurons and in glial cells, are accompanied also by changes in ferritin expression. In fact, in C6 glial cells steady-state level and synthesis of ferritin increased early during OGD, in accordance with the decrease of IRP1 RNA-binding activity. The further increase in ferritin biosynthesis observed at 3 h of reoxygenation is not reflected in a corresponding increase in the protein steady-state levels at this time, suggesting that ferritin half-life could be decreased during the early phase of reoxygenation. The prolonged reoxygenation did not cause a further increase of biosynthesis and steady-state levels of ferritin, in accordance with the recovery of IRP1 binding activity. In these cells, the transcriptional control on ferritin expression does not seem to operate since there were no changes in H-ferritin mRNA levels and therefore, ferritin expression is regulated by the more rapid post-transcriptional mechanism operated by IRPs.

In type-1 astrocytes transcriptional and post-transcriptional mechanisms seem to operate in a different way during OGD and OGD/reoxygenation phases in order to maintain high ferritin levels. In fact, during OGD H-ferritin mRNA levels were decreased and the increased ferritin expression was IRP-dependent. During the early

reoxygenation phase ferritin expression seemed to be dependent by a coupled transcriptional and post-transcriptional control, since H-ferritin mRNA was increased and IRP1 binding activity was low. Also in this case, it can not be excluded that ferritin half-life could be decreased during this phase. During the prolonged reoxygenation phase, in accordance with the increased level of H-ferritin mRNA, the transcriptional control seemed to be the only operating mechanism to maintain high ferritin content, since IRP1 binding activity returned to basal levels.

Conversely, in cortical neurons ferritin expression increased only during the late reoxygenation phase when the IRP1 activity returned to basal level. However, it should be noted that after 3 hr of reoxygenation ferritin synthesis was increased, when protein and mRNA steady-state levels were unchanged, and IRP1 binding activity, although in a declining phase, was still elevated. This apparent discrepancy between increased ferritin synthesis, a sustained IRP-binding activity and no change in mRNA content, can be due to the activation of the protein synthesis machinery that more efficiently translates the ferritin mRNAs present in the cell. In addition, it is possible that the increase in ferritin synthesis cannot be detected by the Western blot analysis as consequence of a decreased

ferritin half-life during the early reoxygenation phase. The significant increase of ferritin levels at 24 h of reoxygenation seems to be mainly regulated at transcriptional level since Northern-blot analysis demonstrated a marked increase of H-ferritin mRNA at this time. This latter result is in agreement with report showing a significant induction of ferritin gene transcription following cerebral ischemia/reperfusion (Chi *et al.*, 2000). The transcriptional regulation of H-ferritin observed during reoxygenation, that implicates an increase in relative amount of this subunit, could reflect the need of an increased iron storage and is consistent with the concept that cells are responding to the stress by increasing the H-ferritin (Theil, 1987). Since neurons and glia have a different susceptibility to oxidative stress caused by hypoxia/reoxygenation (Rosenblum, 1997), the different regulation of ferritin expression may help to explain the diverse vulnerability of neurons and glial cells to OGD/reoxygenation injury. In fact, exposure of neurons to OGD/reoxygenation determined impairment of mitochondrial activity, marked lipid peroxidation and apoptosis. Under the same experimental conditions, glial cells did not show any appreciable reduction in cell viability, lipid peroxidation or apoptosis. The response of neurons can be explained considering that the increased

IRP1 binding activity during OGD determines a reduced ferritin synthesis and an induction of transferrin receptor expression, which could expand the intracellular labile iron pool (Tacchini *et al.*, 1997) and enhance oxidative damage that the delayed ferritin synthesis during reoxygenation is unable to counteract. Conversely, in glial cells the down-regulation of IRP1 binding activity during the OGD could facilitate iron sequestration into ferritin and prevent the oxidative damage due to the formation of the highly reactive oxygen species. Moreover, the results obtained with exogenously added apoferritin to cortical neurons demonstrated that ferritin decreased the OGD/reoxygenation-induced lipid peroxidation, thus suggesting that ferritin acts as a cytoprotective agent by limiting the ability of intracellular iron to generate ROS. Of course, the cytoprotective role exerted by exogenous ferritin is appreciable only during the reoxygenation phase, when the oxygen availability promotes the iron-induced ROS production. Therefore, the earlier ferritin synthesis increase observed in glial cells may represent an adaptive response to oxidative stress generated by OGD/reoxygenation explaining their reduced vulnerability to anoxic insults.

Interestingly, in the *in vivo* model of brain ischemia induced by pMCAO, there was an early and brief increase in IRP1 binding

activity followed by a prolonged reduction in the ischemic core, whereas ferritin expression was slightly reduced. Although the pMCAO experiments are related to total brain tissue, these findings suggest that also *in vivo* cerebral ischemia alters IRP RNA-binding activity and ferritin expression. However, the pMCAO-induced changes in the IRP-IRE complex formation were not associated with the changes in ferritin levels, thus suggesting that such other regulatory events as increased ferritin degradation, could override the effects of IRP-IRE interaction to control steady-state ferritin levels during prolonged ischemia.

It is conceivable that besides being directly regulated by IRPs, ferritin can be indirectly modulated by other factors activated during hypoxia/reoxygenation. In fact, the hypoxia-inducible factor-1 (HIF-1) that induces the expression of several genes including those involved in iron metabolism, i.e., transferrin, transferrin receptor and heme oxygenase-1 (Semenza, 2000), may contribute to the regulation of iron homeostasis. In fact, under the oxidative stress of hypoxia/reperfusion, heme oxygenase-1 is induced and cleaves the heme porphyrin ring releasing Fe^{2+} that in turn may induce ferritin expression.

In conclusion, the results reported in this thesis demonstrate that IRPs RNA-binding activity and ferritin biosynthesis are oppositely regulated in cortical and glial cells exposed to an experimental condition that mimics brain ischemia. The changes observed may be viewed as an adaptive response of the cell to the iron homeostasis dysregulation induced by hypoxia/reoxygenation.

In the light of data on cross-talk between glial and neuronal cells (Bezzi *et al.*, 2001) and our results, it is feasible that when neurons and glial cells are exposed to hypoxia/reoxygenation, glial cells by the early increase in ferritin, which is able to sequester iron, might indirectly protect neurons from the metal-induced injury.

7. REFERENCES

- Abbound, S., Haile, D. J. (2000) A novel mammalian iron-regulated protein involved in intracellular iron metabolism. *J. Biol. Chem.* **275**, 19906-19912
- Allikmets, R., Raskind, W. H., Hutchinson, A., Schueck, N. D., Dean, M., Koeller, D. M., (1999) Mutation of a putative mitochondrial iron transporter gene (ABC7) in X-linked sideroblastic anemia and ataxia (XLSA/A). *Hum. Mol. Genet.* **8**, 743-749
- Andersen, O., Pantopoulos, K., Kao, H. T., Muckenthaler, M., Youson, J. H., Pieribone, V., (1998) Regulation of iron in the sanguivore lamprey *Lampetra fluviatilis*-molecular cloning of two ferritin subunits and two iron regulatory proteins (IRP) reveals evolutionary conservation of the iron-regulatory element (IRE)/IRP regulatory system. *Eur. J. Biochem.* **254**, 223-229
- Arosio, P., Yokota, M., Drysdale, J. W., (1976) Structural and immunological relationships of iso-ferritins in normal and malignant cells. *Cancer Res.* **36**, 1735-1739
- Balla, Jacob H.S., Balla, J., Rosenberg, M., Nath, K., Apple, F., Eaton, J.W. Vercellotti, G.M. (1992) Ferritin: a cytoprotective antioxidant strategem of endothelium. *J. Biol. Chem.* **267**, 18148-18153.
- Brazzolotto, X., Gaillard, J., Pantopoulos, K., Hentze, M. W., Moulis, J. M., (1999) Human cytoplasmic aconitase (Iron regulatory protein 1) is converted into its [3Fe-4S] form by hydrogen peroxide in vitro but is not activated for iron-responsive element binding. *J. Biol. Chem.* **274**, 21625-21630.
- Beard, J. L., Connor, J. R., Jones, B. C. (1993) Iron in the brain. *Nutr. Rev.* **51**, 157-170
- Beinert, H., Kennedy, M. C., (1993) Aconitase, a two-faced protein: enzyme and iron regulatory factor. *FASEB J.* **7**, 1442-1449

- Bemis, L., Chan, D. A., Finkielstein, C. V., Qi, L., Sutphin, P. D., Chen, X., Stenmark, K., Giaccia, A. J., Zundel, W., (2004) Distinct aerobic and hypoxic mechanisms of HIF-alpha regulation by CSN5. *Genes Dev.* **18**, 739-744
- Benkovic, S. A., Connor, J. R., (1993) Ferritin, transferrin, and iron in selected regions of the adult and aged rat brain. *J. Comp. Neurol.* **338**, 97-113
- Bezzi, P., Domercq, M., Vesce, S., Volterra, A. (2001) Neuron-astrocyte cross-talk during synaptic transmission: physiological and neuropathological implications. *Prog. Brain Res.* **132**, 255-265
- Bolann, B. J., Ulvik, R. J. (1987) Release of iron from ferritin by xanthine oxidase. *Biochem. J.* **243**, 55-59
- Bothwell TH., (1995) Overview and mechanisms of iron regulation. *Nutr. Rev.* **53**, 237-45
- Bouton, C., Hirling, H., Drapier, J.C. (1997) Redox modulation of iron regulatory proteins by peroxynitrite. *J. Biol. Chem.* **272**, 19969-19975
- Bradbury, M. W. B., (1997) Transport of iron in the blood-brain-cerebrospinal fluid system. *J. Neurochem.* **69**, 443-451
- Burdo, J. R., Menzies, S. L., Simpson, I. A., Garrick, L. M., Garrick, M. D., Dolan, K. G., Haile, D. J., Beard, J. L., Connor, J. R., (2001) Distribution of divalent metal transporter 1 and metal transport protein 1 in the normal and Belgrade rat. *J. Neurosci Res.* **66**, 1198-207
- Cairo, G., Pietrangelo, A., (2000) Iron regulatory proteins in pathobiology. *Biochem J.* **352**, 241-50
- Cairo, G., Recalcati, S., Pietrangelo, A., Minotti, G., (2002) The iron regulatory proteins: targets and modulators of free radical reactions and oxidative damage. *Free Radic. Biol.* **32**, 1237-43
- Campbell, D. R., Skikne, B. S., Cook, J. D., (1986) Cerebrospinal fluid ferritin levels in screening for meningism. *Arch. Neurol.* **43**, 1257-1260

Cheepsunthorn, P., Palmer, C., Menzies, S., Roberts, R. L., Connor, J. R., (2001) Hypoxic/ischemic insult alters ferritin expression and myelination in neonatal rat brains. *J. Comp. Neurol.* **431**, 382-396

Chen, Q., Beard, J.L., Jones, B.C. (1995) Abnormal rat brain monoamine metabolism in iron deficiency anemia. *J. Nutr. Biochem.* **6**, 486-493

Chen, D., Li, M., Luo, J., Gu, W., (2003) Direct interactions between HIF-1 alpha and Mdm2 modulate p53 function. *J. Biol. Chem.* **278**, 13595-13598

Chi, S. I., Wang, C. K., Chen, J. J., Chau, L. Y., Lin, T. N., (2000) Differential regulation of H and L ferritin messenger RNA subunit, ferritin protein and iron following focal cerebral ischemia-reperfusion. *Neuroscience* **100**, 475-484

Chomczynski, P., Sacchi, N., (1987) Single-step method of RNA isolation by acid guanidinium thiocyanate-phenol-chloroform extraction. *Anal Biochem.* **162**,156-159

Connor, J.R., Menzies, S.L. (1996) Relationship of iron to oligodendrocytes and myelination. *Glia* **17**, 83-93

Connor, J. R., (1994) Iron regulation in the brain at the cell and molecular level. *Adv. Exp Med. Biol.* **356**, 229-238

Cramer, T., Yamanishi, Y., Clausen, B. E., Forster, I., Pawlinski, R., Mackman, N., Haase, V. H., Jaenisch, R., Corr, M., Nizet, V., Firestein, G. S., Gerber, H. P., Ferrara, N., Johnson, R. S., (2003) HIF-1alpha is essential for myeloid cell-mediated inflammation. *Cell.* **112**, 645-657

Donovan, A., Brownlie, A., Zhou, Y., Shepard, J., Pratt, S. J., Moynihan, J., Paw, B. H., Drejer, A., Barut, B., Zapata, A., Law, T. C., Brugnara, C., Lux, S. E., Pinkus, G. S., Pinkus, J. L., Kingsley, P. D., Palis, J., Fleming, M. D., Andrews, N.C., Zon, L. I., (2000) Positional cloning of zebrafish ferroportin1 identifies a conserved vertebrate iron exporter. *Nature.* **403**, 776-781

Dorrepaal, C.A., Berger, H.M., Benders, M.J., van Zoeren-Grobbe, D., van de Bor, M., van Bel, F. (1996) Nonprotein-bound iron in postasphyxial reperfusion injury of the newborn. *Pediatrics* **98**, 883-889.

Eisenstein, R. S., Blemings, K. P., (1998) Iron regulatory proteins, iron responsive elements and iron homeostasis. *J. Nutr.* **128**, 2295-2298

Eisenstein R. S., (2000) Discovery of the ceruloplasmin homologue hephaestin: new insight into the copper/iron connection. *Nutr. Rev.* **58**, 23-27

Ema, M., Taya, S., Yokotani, N., Sogawa, K., Matsuda, Y., Fujii-Kuriyama, Y. (1997) A novel bHLH-PAS factor with close sequence similarity to hypoxia-inducible factor 1 α regulates the VEGF expression and is potentially involved in lung and vascular development. *Proc. Natl. Acad. Sci. USA.* **94**, 4273-4278

Esterbauer, H., Cheeseman, K. H., (1990) Determination of aldehydic lipid peroxidation products: malonaldehyde and 4-hydroxynonenal. *Methods Enzymol.* **186**, 407-421

Fandrey, J., Frede, S., Jelkmann, W., (1994) Role of hydrogen peroxide in hypoxia-induced erythropoietin production. *Biochem. J.* **303**, 507-510

Faucheux, B.A., Nillesse, N., Damier, P., Spik, G., Mouatt-Prigent, A., Pierce, A., Leveugle, B., Kubis, N., Hauw, J. J., Agid, Y., (1995) Expression of lactoferrin receptors is increased in the mesencephalon of patients with Parkinson disease. *Proc. Natl. Acad. Sci.* **92**, 9603-7

Ferriera, C., Bucchini, D., Martin, M. E., _Levi S, Arosio P, Grandchamp B, Beaumont C_ (2000) Early embryonic lethality of H ferritin gene deletion in mice. *J. Biol. Chem.* **275**, 3021-3024

Festa, M., Colonna, A., Pietropaolo, C., Ruffo, A. (2000a) Oxalomalate, a competitive inhibitor of aconitase, modulates the RNA-binding activity of iron-regulatory proteins. *Biochem. J.* **348**, 315-320

Festa, M., Ricciardelli, G., Mele, G., Pietropaolo, C., Ruffo, A., Colonna, A. (2000b) Overexpression of H-ferritin and up-regulation

of iron regulatory protein genes during differentiation of 3T3-L1 pre-adipocytes. *J. Biol. Chem.* **275**, 36708-36712

Fishman, J.B., Rubin, J.B., Handrahan, J.V., Connor, J.R., Fine, R.E. (1987) Receptor mediated transcytosis of transferrin across the blood-brain barrier. *J. Neurosci. Res.* **18**, 299-304

Fox, S. B., Braganca, J., Turley, H., Campo, L., Han, C., Gatter, K. C., Bhattacharya, S., Harris, A. L. (2004) CITED4 inhibits hypoxia-activated transcription in cancer cells, and its cytoplasmic location in breast cancer is associated with elevated expression of tumor cell hypoxia-inducible factor 1alpha. *Cancer Res.* **64**, 6075-6081

Gerlach, M., Ben-Shachar, D., Riederer, P., Youdim, M. B., (1994) Iron regulates cytoplasmic levels of a novel iron-responsive element-binding protein without aconitase activity. *J. Biol. Chem.* **269**, 24252-24260

Goessling, L. S., Mascotti, D. P., Thach, R. E., (1998) Involvement of heme in the degradation of iron-regulatory protein 2. *J. Biol. Chem.* **273**, 12555-12557

Goetz, D. H., Holmes, M.A., Borregaard, N., Bluhm, M. E., Raymond, K. N., Strong, R. K., (2002) The neutrophil lipocalin NGAL is a bacteriostatic agent that interferes with siderophore-mediated iron acquisition. *Mol Cell.* **10**, 1033-43

Goldberg, M., Choi, D. W., (1993) Combined oxygen and glucose deprivation in cortical cell culture: calcium-dependent and calcium-independent mechanism of neuronal injury. *J. Neurosci.* **13**, 3510-3524

Gu, Y. Z., Moran, S. M., Hogenesch, J. B., Wartman, L., Bradfield, C. A., (1998) Molecular characterization and chromosomal localization of a third alpha-class hypoxia inducible factor subunit, HIF3alpha. *Gene Expr.* **7**, 205-213

Guo, B., Yu, Y., Leibold, E.A. (1994) Iron regulates cytoplasmic levels of a novel iron-responsive element-binding protein without aconitase activity. *J. Biol. Chem.* **269**, 24252-24260

Halliwell, B., Gutteridge, J.M. (1990) The role of free radicals and catalytic metal ions in human disease: an overview. *Methods Enzymol.* **186**, 1-85

Halliwell B., (1992) Reactive oxygen species and the central nervous system. *J. Neurochem.* **59**, 1609-1623

Hanson, E. S. Leibold, E. A., (1998) Regulation of iron regulatory protein 1 during hypoxia and hypoxia/reoxygenation. *J. Biol. Chem.* **273**, 7588-7593

Hanson, E. S., Foot, L. M., Leibold, E. A. (1999) Hypoxia post-translationally activates iron-regulatory protein 2. *J. Biol. Chem.* **274**, 5047-5052

Hanson, E.S, Rawlins, M.L., Leibold, E.A. (2003) Oxygen and iron regulation of iron regulatory protein 2. *J. Biol. Chem.* **278**, 40337-40342

Hara, S., Hamada, J., Kobayashi, C., Kondo, Y., Imura, N., (2001) Expression and characterization of hypoxia-inducible factor (HIF)-3 α in human kidney: suppression of HIF-mediated gene expression by HIF-3 α . *Biochem. Biophys Re. Commun.* **287**, 808-813

Harrison, P.M., Arosio, P. (1996) The ferritins: molecular properties, iron storage function and cellular regulation. *Biochim. Biophys. Acta* **1275**, 161-203

Hentze, M.W., Rouault, T.A., Harford, J.B., Klausner, R.D. (1989) Oxidation-reduction and the molecular mechanism of a regulatory RNA-protein interaction. *Science* **244**, 357-359

Hogenesch, J. B., Chan, W. K., Jackiw, V. H., Brown, R. C., Gu, Y. Z., Pray-Grant, M., Perdew, G. H., Bradfield, C. A., (1997) Characterization of a subset of the basic-helix-loop-helix-PAS superfamily that interacts with components of the dioxin signaling pathway. *J. Biol. Chem.* **272**, 8581-8593

Huang, L. E., Gu, J., Schau, M., Bunn, H. F., (1998) Regulation of hypoxia-inducible factor 1 α is mediated by an oxygen dependent domain via the ubiquitin -proteosome pathway. *Proc. Natl. Acad. Sci. USA* **95**, 7987-7992

Hulet, S. W., Hess, E. J., Debinski, W., Arosio, P., Bruce, K., Powers, S., Connor, J. R., (1999a) Characterization and distribution of ferritin binding sites in the adult mouse brain. *J. Neurochem.* **72**, 868-874

Hulet, S. W., Powers, S., Connor, J. R., (1999b) Distribution of transferrin and ferritin binding in normal and multiple sclerotic human brains. *J. Neurol. Sci.* **165**, 48-55

Hulet, S. W., Heyliger, S. O., Powers, S., Connor, J. R., (2000) Oligodendrocyte progenitor cells internalize ferritin via clathrin-dependent receptor mediated endocytosis. *J. Neurosci. Res.* **61**, 52-60

Irace, C., Scorziello, A., Maffettone, C., Pignataro, G., Matrone, C., Adornetto, A., Santamaria, R., Annunziato, L., Colonna, A., (2005) Divergent modulation of iron regulatory proteins and ferritin biosynthesis by hypoxia/reoxygenation in neurons and glial cells. *J. Neurochem.* **95**, 1321-1331

Ischiropoulos, H., Beckman, J. S., (2003) Oxidative stress and nitration in neurodegeneration: cause, effect, or association? *J. Clin. Invest.* **111**, 163-169

Ishimaru, H., Ishikawa, K., Ohe, Y., Takahashi, A., Tatemoto, K., Maruyama, Y. (1996) Activation of iron handling system within the gerbil hippocampus after cerebral ischemia. *Brain Res.* **726**, 23-30

Iwai, K., Drake, S. K., Wehr, N. B., Weissman, A. M., LaVaute, T., Minato, N., Klausner, R. D., Levine, R. L., Rouault, T. A., (1998) Iron-dependent oxidation, ubiquitination, and degradation of iron regulatory protein 2: implications for degradation of oxidized proteins. *Proc Natl Acad Sci USA.* **95**, 4924-4928

Kakhlon, O., Gruenbaum, Y., Cabantchik, Z. I., (2001) Repression of the heavy ferritin chain increases the labile iron pool of human K562 cells. *Biochem. J.*, **356**, 311-316

Ke, Y., Ming Qian, Z. (2003) Iron misregulation in the brain: a primary cause of neurodegenerative disorders. *Lancet Neurology* **2**, 246-253

Keir,, G., Tasdemir, N., Thompson, E. J., (1993) Cerebrospinal fluid ferritin in brain necrosis: evidence for local synthesis. *Clin. Chim. Acta* **216**, 153-166

Kennedy, M.C., Mende-Mueller, L., Blondin, G.A., Beinert, H. (1992) Purification and characterization of cytosolic aconitase from beef liver and its relationship to the iron-responsive element binding protein. *Proc. Natl. Acad. Sci. USA* **89**, 11730– 11734

Kondo, Y., Ogawa, N., Asanuma, M., Ota, Z., Mori, A. (1995) Regional differences in late-onset iron deposition, ferritin, transferrin, astrocyte proliferation and microglia activation after transient forebrain ischemia in rat brain. *J. Cereb. Blood Flow. Metab.* **15**, 216-226

Kondo, T., Shirasawa, T., Itoyama, Y., Mori, H., (1996) Embryonic genes expressed in Alzheimer's disease brains. *Neurosci Lett.* **209**, 157-160

Konijn, A. M., Glickstein, H., Vaisman, B., Meyron-Holtz, E. G., Slotki, I. N., Cabantchik, Z. I. (1999) The cellular labile iron pool and intracellular ferritin in K562 cell. *Blood* **94**, 2128-2134

Knight, S. A. B., Babu, N., Sepuri, V., Pain, D., Dancis, A. (1998) Mt-Hsp70 homolog, Ssc2p, required for maturation of yeast frataxin and mitochondrial iron homeostasis. *J. Biol. Chem.* **273**, 18839-18893

Kuriyama-Matsumura, K., Sato, H., Suzuki, M., Banai, S., (2001) Effects of hyperoxia and iron on iron regulatory protein-1 activity and ferritin synthesis in mouse peritoneal macrophages. *Biochim. Biophys Acta Protein Struct. Mol. Enzymol.* **1544**, 370-377

Lange, H., Kispal, G., Lill, R. (1999) Mechanism of iron transport to the site of heme synthesis inside yeast mitochondria. *J. Biol. Chem.* **274**, 18989-18996

LaVaute, T., Smith, S., Cooperman, S., Iwai, K., Land, W., Meyron-Holtz, Drake, S. K., Miller, G., Abu-Asab, M., Tsokos, M., Switzer III, R., Grinberg, A., Love, P., Tresser, N., Rouault, T. A., (2001) Targeted deletion of the gene encoding iron regulatory protein-2 causes

misregulation of iron metabolism and neurodegenerative disease in mice. *Nat. Genet.* **27**, 209-214

Lawson, D. M., Treffry, A., Artymiuk, P. J., Harrison, P. M., Yewdall, S. J., Luzzago, A., Cesareni, G., Levi, S., Arosio, P., (1989) Identification of the ferroxidase centre in ferritin. *FEBS Lett.* **254**, 207-210

Leibold, E.A., Gahring, L.C., Rogers, S.W. (2001) Immunolocalization of iron regulatory protein expression in the murine central nervous system. *Histochem. Cell. Biol.* **115**, 195-203

Levi, S., Corsi, B., Bosisio, M., Invernizzi, R., Volz, A., Sanford, D., Arosio, P., Drysdale, J., (2001) A human mitochondrial ferritin encoded by an intronless gene. *J Biol Chem.* **276**, 24437-24440

Levy, J. E., Jin, O., Fujiwara, Y., Kuo, F., Andrews, N. C., (1999) Transferrin receptor is necessary for development of erythrocytes and the nervous system. *Nat. Genet.* **21**, 396-399

Le Vine, S. M., Lynch, S. G., Ou, C. N., Wulser, M. J., Tam, E., Boo, N., (1999) Ferritin, transferrin and iron concentrations in the cerebrospinal fluid of multiple sclerosis patients. *Brain Res.*, **821**, 511-515

Linert, W., Jameson, G. N., (2000) Redox reactions of neurotransmitters possibly involved in the progression of Parkinson's Disease. *J. Inorg. Biochem.* **79**, 319-26

Malecki, E. A., Devenyi, A. G., Beard, J. L., Connor, J. R., (1999) Existing and emerging mechanisms for transport of iron and manganese to the brain. *J. Neurosci Res.* **56**, 113-122

Maxwell, P. H., Wiesener, M. S., Chang, G. W., Clifford, S. C., Vaux, E. C., Cockaman, M. E., Wykoff, C. C., Pugh, C. W., Maher, E. R., Ratcliffe, P. J., (1999) The tumor suppressor protein VHL targets hypoxia-inducible factors for oxygen-dependent proteolysis. *Nature* **399**, 271-275

McCarthy, K.D., de Vellis, J. (1980) Preparation of separate astroglial and oligodendroglial cell cultures from rat cerebral tissue. *J. Cell. Biol.* **85**, 890-902

McKie, A. T., Marciani, P., Rolfs, A., Brennan, K., Wehr, K., Barrow, D., Miret, S., Bomford, A., Peters, T. J., Farzaneh, F., Hediger, M. A., Hentze, M. W., Simpson, R. J., (2000) A novel duodenal iron-regulated transporter, IREG1, implicated in the basolateral transfer of iron to the circulation. *Mol. Cell.* **5**, 299-309

McKie, A. T., Barrow, D., Latunde-Dada, G. O., Rolfs, A., Sager, G., Mudaly, E., Mudaly, I., Richardson, C., Barlow, D., Bomford, A., Peters, T. J., Raja, K. B., Shirali, S., Hediger, M. A., Farzaneh, F., Simpson, R. J., (2001) An iron-regulated ferric reductase associated with the absorption of dietary iron. *Science* **291**, 1755-1759

Meyron-Holtz, E.G., Ghosh, M.C., Rouault, T.A. (2004) Mammalian tissue oxygen levels modulate iron-regulatory protein activities in vivo. *Science* **306**, 2087-2090

Moos, T., Morgan, E. H., (1998) Evidence for low molecular weight, non-transferrin-bound iron in rat brain and cerebrospinal fluid. *J. Neurosci Res.* **54**, 486-94

Morris, C. M., Candy, J. M., Keith, A. B., Oakley, A. E., Taylor, G. A., Pullen, R. G. L., Bloxham, C. A., Gocht, A., Edwardson, J. A., (1992) Brain iron homeostasis. *J. Inorg. Biochem.* **47**, 257-265

Neilands, JB. (1991) A brief history of iron metabolism. *Biol. Met.* **4**, 1-6

Oshiro, S., Kawahara, M., Kuroda, Y., Zhang, C., Cai, Y., Kitajima, S., Shirao, M., (2000). Glial cells contribute more to iron and aluminum accumulation but are more resistant to oxidative stress than neuronal cells. *Biochim. Biophys Acta.* **1502**, 405-414

Pantopoulos, K., Hentze, M. W., (1995) Rapid responses to oxidative stress mediated by iron regulatory protein. *EMBO J.* **14**, 2917-2924

Pantopoulos, K. (2004) Iron metabolism and the IRE/IRP regulatory system. An update. *Ann. N.Y. Acad. Sci.* **1012**, 1-13

- Picard, V., Epsztejn, S., Santambrogio, P., Cabantchik, Z. I., Beaumont, C., (1998) Role of ferritin in the control of the labile iron pool in murine erythroleukemia cells. *J. Biol. Chem.* **273**, 15382-125386
- Pinero, D., Li, N. Q., Connor, J. R., Beard, J. L., (2000) Variations in dietary iron alter brain iron metabolism in developing rats. *J. Nutr.* **130**, 254-263
- Ponka, P. (1997) Tissue-specific regulation of iron metabolism and heme synthesis: distinct control mechanisms in erythroid cells. *Blood* **90**, 473-474
- Ponka, P., Beaumont, C., Richardson, D. R., (1998) Function and regulation of transferrin and ferritin. *Semin. Hematol.* **35**, 35-54
- Qi, Y., Jamindar, T. M., Dawson, G., (1995) Hypoxia alters iron homeostasis and induces ferritin synthesis in oligodendrocytes. *J. Neurochem.* **64**, 2458-2464
- Rolfs, A., Kvietikova, I., Gassmann, M., Wenger, R. H., (1997) Oxygen-regulated transferrin expression is mediated by hypoxia-inducible factor 1. *J. Biol. Chem.* **272**, 20055-20062
- Rosenblum, W.I. (1997) Histopathologic clues to the pathways of neuronal death following ischemia/hypoxia. *J. Neurotrauma* **14**, 313-326
- Rouault, T. A., Tang, C. K., Kaptain, S., Burgess, W. H., Haile, D. J., Samaniego, F., McBride, O. W., Harford, J. B., Klausner, R. D., (1990) Cloning of the cDNA encoding an RNA regulatory protein- the human iron-responsive element-binding protein. *Proc. Natl. Acad. Sci. USA* **87**, 7958-7962
- Rucker, P., Torti, F. M., Torti, S. V., (1996) Role of H and L subunits in mouse ferritin. *J. Biol. Chem.* **271**, 33352-33357
- Ryter, S. W., Tyrrell, R. M., (2000) The heme synthesis and degradation pathways: role in oxidant sensitivity. Heme oxygenase has both pro-and antioxidant properties. *Free Radical Biol. Med.* **28**, 289-309

Santambrogio, P., Cozzi, A., Levi, S., Arosio, P., (1987) Human serum ferritin G-peptide is recognized by anti-L ferritin subunit antibodies and concanavalin-A. *Br. J. Haematol.* **65**, 235-237

Schneider, B.D., Leibold, E.A. (2003) Effects of iron regulatory protein regulation on iron homeostasis during hypoxia. *Blood* **102**, 3404-3411

Scorziello, A., Pellegrini C., Forte L., Tortiglione A., Gioielli A., Iossa S., Amoroso S., Tufano R., Di Renzo G., Annunziato L. (2001) Differential vulnerability of cortical and cerebellar neurons in primary culture to oxygen glucose deprivation followed by reoxygenation. *J. Neurosci. Res.* **63**, 20-26

Semenza, G. L., Agani, F., Booth, G., Forsythe, J., Iyer, N., Jiang, B. H., Leung, S., Roe, R., Wiener, C., Yu, A., (1997). Structural and functional analysis of hypoxia-inducible factor 1. *Kidney Int.* **51**, 553-555

Semenza, G.L., (2000) Surviving ischemia: adaptive responses mediated by hypoxia-inducible factor 1. *J. Clin. Invest.* **106**, 809-812

Siddappa, A.J., Rao, R.B., Wobken, J.D., Leibold, E.A., Connor, J.R., Georgieff, M.K. (2002) Developmental changes in the expression of iron regulatory proteins and iron transport proteins in the perinatal rat brain. *J. Neurosci. Res.* **68**, 761-775

Simpson, R. J., (1996) Dietary iron levels and hypoxia independently affect iron absorption in mice. *J. Nutr.* **126**, 1858-1864

Sindic, C. J., Collet-Cassart, D., Masson, P. L., Laterre, E. C., (1981) The clinical relevance of ferritin concentration in the cerebrospinal fluid. *J. Neurol. Neurosurg. Psych.* **44**, 329-333

Sipe, D. M., Murphy, R. F., (1991) Binding to cellular receptors results in increased iron release from transferrin at mildly acidic pH. *J. Biol. Chem.* **266**, 8002-8007

Soum, E., Brazzolotto, X., Goussias, C., Bouton, C., Moulis, J. M., Mattioli, T. A., Drapier, J. C., (2003) Peroxynitrite and nitric oxide

differently target the iron-sulfur cluster and amino acid residues of human iron regulatory protein 1. *Biochemistry* **42**, 7648-7254

Tacchini, L., Recalcati, S., Bernelli-Zazzara, A., Cairo, G., (1997) Induction of ferritin synthesis in ischemic-reperfused rat liver: analysis of the molecular mechanisms. *Gastroenterology*. **113**, 946-953

Tacchini, L., Bianchi, L., Bernelli-Zazzera, A., Cairo, G., (1999) Transferrin receptor induction by hypoxia. *J. Biol. Chem.* **274**, 24142-24146

Tacchini, L., Fusar Poli, D., Bernelli-Zazzera, A., Cairo, G., (2002) Transferrin receptor gene expression and transferrin-bound iron uptake are increased during postischemic rat liver reperfusion. *Hepatology* **36**, 103-111

Theil, E.C. (1987) Ferritin: structure, gene regulation, and cellular function in animals, plants, and microorganisms. *Annu. Rev. Biochem.* **56**, 289-315

Thomson, A. M., Rogers, J. T., Leedman, P. J. (1999) Iron-regulatory proteins, iron-responsive elements and ferritin mRNA translation. *Int. J. Biochem. Cell Biol.* **31**, 1139-1152

Thompson, K.J., Shoham, S., Connor, J.R. (2001) Iron and neurodegenerative disorders. *Brain Res. Bull.* **55**, 155-164

Tian, H., McKnight, S. L., Russell, D. W., (1997) Endothelial PAS domain protein 1 (EPAS1), a transcription factor selectively expressed in endothelial cells. *Genes Dev.* **11**, 72-82

Toth, I., Yuan, L. P., Rogers, J. T., Boyce, H., Bridges, K. R., (1999) Hypoxia alters iron-regulatory protein-1 binding capacity and modulates cellular iron homeostasis in human hepatoma and erythroleukemia cells. *J. Biol. Chem.* **274**, 4467-4473

Tortiglione, A., Minale, M., Pignataro, G., Amoroso, S., Di Renzo, G., Annunziato, L. (2002) The 2-oxopyrrolidinacetamide piracetam reduces infarct brain volume induced by permanent middle cerebral artery occlusion in male rats. *Neuropharmacology* **43**, 427-433

Torti, S. V., Torti, F. M., (1994) Iron and ferritin in inflammation and cancer. *Adv. Inorg. Biochem.* **10**, 119-137

Torti, S. V., Kwak, E. L., Miller, S. C., Miller, L. L., Ringold, G. M., Myambo, K. B., Young, A. P., Torti, F. M., (1988) The molecular cloning and characterization of murine ferritin heavy chain, a tumor necrosis factor-inducible gene. *J. Biol. Chem.* **263**, 12638-12644

Vulpe, C. D., Kuo, Y. M., Murphy, T. L., Cowley, L., Askwith, C., Libina, N., Gitschier, J., Anderson, G. J., (1999) Hephaestin, a ceruloplasmin homologue implicated in intestinal iron transport, is defective in the sla mouse. *Nat Genet.* **21**, 195-199

Wang, G. L., Jiang, B. H., Rue, E. A., Semenza, G. L., (1995) Hypoxia-inducible factor 1 is a basic-helix-loop-helix-PAS heterodimer regulated by cellular O₂ tension. *Proc. Natl. Acad. Sci. USA.* **92**, 5510-5514

Wenger, R. H., (2002) Cellular adaptation to hypoxia: O₂-sensing protein hydroxylases, hypoxia-inducible transcription factors, and O₂-regulated gene expression. *FASEB J.* **16**, 1151-1162

Wiesener, M. S., Turley, H., Allen, W. E., Willam, C., Eckardt, K. U., Talks, K. L., Wood, S. M., Gatter, K. C., Harris, A. L., Pugh, C. W., Ratcliffe, P. J., Maxwell, P. H., (1998) Induction of endothelial PAS domain protein-1 by hypoxia: characterization and comparison with hypoxia-inducible factor-1 α . *Blood* **92**, 2260-2268

Yang, J., Goetz, D., Li, J. Y., Wang, W., Mori, K., Setlik, D., Du, T., Erdjument-Bromage, H., Tempst, P., Strong, R., Barasch, J., (2002) An iron delivery pathway mediated by a lipocalin. *Mol Cell.* **10**, 1045-1056

Yeh, K. Y., Yeh, M., Glass, J., (1998) Expression of intestinal brush-border membrane hydrolases and ferritin after segmental ischemia-reperfusion in rats. *Am. J. Physiol. Gastrointest. Liver Physiol.* **38**, 572-583

Zappone, E., Bellotti, V., Cazzola, M., Ceroni, M., Meloni, F., Pedrazzoli, P., Perfetti, V., (1986) Cerebrospinal fluid ferritin in human disease. *Haematologica* **71**, 103-107

